UNIVERSITY OF OKLAHOMA GRADUATE COLLEGE

INVESTIGATING CLIMATE IMPACTS ON WEATHER-RELATED CRASHES

A THESIS
SUBMITTED TO THE GRADUATE FACULTY
in partial fulfillment of the requirements for the
Degree of

MASTER OF SCIENCE

By

AYMAN ELYOUSSOUFI
Norman, Oklahoma

2025

INVESTIGATING CLIMATE IMPACTS ON WEATHER-RELATED CRASHES

A THESIS APPROVED FOR THE SCHOOL OF METEOROLOGY

BY THE COMMITTEE CONSISTING OF

Dr. Kathy Pegion, Chair

Dr. Brad Illston

Dr. Curtis Walker

TABLE OF CONTENTS

LIST OF TABLES

LIST OF FIGURES

ABSTRACT

Adverse weather conditions due to precipitation are known to increase crash occurrence and fatality rates. One fifth of all vehicle crashes in the United States are weather-related, with a sixth of this value resulting in a fatality. However, the impacts vary by precipitation type and region. Weather regimes, which identify large-scale atmospheric patterns, are useful to study for accounting region-specific precipitation variability. This study examined the relationship between fatal weather-related crashes and ENSO-precipitation-anomaly and weather-related crashes and regime-precipitation-anomaly time scales to better understand subseasonal-to-seasonal variability in weather impacts to surface transportation and safety communication. Fatal crash, precipitation, snow, and weather regime data were combined to determine how strong climate impacts are to roads. Two important takeaways from this study are that: (1) the precipitation anomalies and fatal crash relationship is driven by anomalous liquid precipitation rather than anomalous snow or frozen precipitation and (2) weather regimes impact fatal weather-related crashes differently from region to region. Traffic safety has improved over time in terms of safety, though climate change may alter future trends. El Niño-Southern Oscillation (ENSO) patterns influence precipitation in some regions, which can affect crash rates, though direct links remain uncertain. Many fatal crashes occur without any prior warnings, indicating a need for improved safety communication to drivers about the dangers of adverse weather. Since climatology and driver behavior differ regionally, crash counts vary. Limitations include the lack of availability of earlier frozen precipitation data and non-fatal weather-related crash data.

CHAPTER 1: INTRODUCTION

One-fifth of all vehicle crashes and 16% of fatal vehicle crashes in the United States are due to weather according to the Federal Highway Administration (FHWA 2025). Vehicle crashes are caused by a variety of factors, including human error, mechanical defects, and environmental conditions such as non-dry pavement conditions (Pisano et al. 2008; Stevens et al. 2019). Adverse weather conditions such as rain, snow, and ice reduce visibility and make the road surface slippery. This increases the occurrence of not only losing control of one's vehicle, but also being involved in a collision with another vehicle (Stevens et al. 2019). Snow and ice reduce tire friction, which makes it difficult to control vehicles. The impact of weather on crash occurrence is further complicated by human error and behavior. Lower vehicle volume at night inhibits the occurrence of being involved in a weather-related crash with another vehicle, so most crashes that do occur at night are a result of poor lighting or traffic violations such as speeding (Fountas et al. 2020, Obeidat et al. 2024). Even then, some drivers underestimate the occurrences of weather conditions, such as rain, further elevating the number of weather-related crashes throughout the day (Pisano et al. 2008; Black and Mote 2015; Saha et al. 2016; Tobin et al. 2019; Tobin et al. 2021; Tobin et al. 2022; Elyoussoufi et al. 2023). While snow was shown to net less crash fatalities than rain, the first snow event of the year frequently holds the highest crash occurrence (Eisenberg and Warner 2005). Similarly, the first rainfall event after a prolonged period of dry conditions also yielded a higher crash occurrence (Lobo et al. 2019). Crash occurrences can remain elevated after a rain or snow event because hazardous pavement conditions can last for days. Understanding these weather-related factors is important for improving road safety measures, enhancing weather warning systems, and notifying drivers about the hazards associated with different weather conditions.

Nearly three-fourths of weather-related crashes in the US are due to wet pavement conditions, which is usually the result of rain (FHWA 2024). However, it is important to note that precipitation amounts, frequency, duration, and type vary widely across the US. As a result vehicle crashes due to adverse weather vary significantly from state to state as well. In the southern and south-east portions of the country, the most common precipitation type is rain, so most weather-related crashes in these regions occur due to active rain or wet pavement. For example, 7% of all fatal crashes in the state of Texas during 1982-2011 were due to rain (Jackson and Sharif 2016). Winter precipitation also impacts crash occurrence, which is why a fourth of US winter-related crashes occur in the north-central United States (Andreescu and Frost 1998; Eisenberg and Warner 2005; Pisano et al. 2008; Andrey 2010; Black and Mote 2015; Call et al. 2019; Mills et al. 2019; Call and Flynt 2022). For example, in Wisconsin, the range of annual snowfall can be as little as 76 cm (30 in) to as much as 254 cm (100 in) for the state. When taking this into account with its continental climate and very cold winters, hazards due to winter precipitation can persist for several days at a time (Shenghong 2020).

The correlation between vehicle crashes and inclement weather also varies by precipitation type. In fact, active rain has been proven to increase the quantity of fatal weather-related crashes the most compared to other active precipitation types (Pisano et al. 2008; Ashley et al. 2015; Tobin et al. 2019; Tobin et al. 2022; Tobin et al. 2024b; FHWA 2024). This is due to a combination of several factors, such as drivers considering rain to not be a hazardous weather condition and being the most prevalent inclement weather type nationwide (Pisano et al. 2008). Drivers also rarely cancel trips due to rain (Pisano et al. 2008). This is why parameters such as traffic volume and trip duration change marginally during the rain when compared to clear weather (Elyoussoufi et al. 2023). Similarly, many people consider snow to be one of the more hazardous weather types, and therefore often cancel trips or drive slower (Pisano et al. 2008; Elyoussoufi et al. 2023). Other precipitation types such as freezing rain or sleet are typically not as common, which explains why they result in fewer weather-related crashes (Pisano et al. 2008).

A metric called crash factor addresses the likelihood of a crash to occur during certain weather conditions (Tobin et al. 2024a) and is used as a proxy for crash relative occurrence estimates (Black and Mote 2015). Crash factor estimates are based on the odds of crash occurrence during precipitation as opposed to odds of crashes occurring when conditions are normal (Tobin et al. 2024a). Rain was found to have the lowest crash factor but often resulted in higher speed crashes. Conversely, freezing rain had the highest crash factor but crashes occurred at slower speeds and were less severe overall. The crash ratio, a quantity that addresses the question of how many crashes occur during precipitation relative to normal, varies temporally. This ratio was found to be the highest for rain and snow during the evening and morning, respectively. This highlights the overall rise in crash occurrence with any precipitation type.

There has been a downward trend in weather-related crashes, regardless of whether they led to a fatality (Pisano et al. 2008; Jackson and Sharif 2016; Han and Sharif 2020). Findings from the 2000s have observed that one-quarter of all US vehicle crashes were weather-related (Eisenberg and Warner 2005; Pisano et al. 2008). However, now only one-fifth of all US crashes are due to weather (FHWA 2024). While there is a clear decrease in the quantity of crashes due to weather, the percentage of crashes that are a result of wet pavement and rainy conditions remain unchanged (FHWA 2024). Prior to 2010, the percentage of weather-related crashes due to wet pavement conditions was 75% (Pisano et al. 2008). The decline in crashes varies by region because driving and climate conditions, including precipitation, directly affect crashes (Whitelegg 1987; Lasarre 2001; Page 2001; Andrey 2010).

Understanding the relationship between precipitation and vehicle crashes is important for developing targeted strategies in an effort to enhance road safety. Past work has confirmed the significant impact that adverse weather has on vehicle-crashes (Whitelegg 1987; Lasarre 2001; Page 2001; Pisano et al. 2008). This highlights not only the tremendous variability in weather-related crashes but the need for more region-specific research on such matters. By examining how different weather conditions contribute to an increase in crash occurrence, warning systems can be improved and the public can be more informed about the safety occurrences between different precipitation types. Such an approach can help reduce future weather-related crashes and better communicate the occurrence precipitation variability has on these crashes.

One well-known source of precipitation variability on seasonal to interannual timescales is the El Niño Southern Oscillation (ENSO) (Du et al. 2020; Kim et al. 2021, Huang and Stevenson 2023). ENSO is a large-scale coupled ocean-atmosphere phenomena that involves fluctuating sea surface temperature (SST) anomalies in the eastern and central Pacific Ocean (Trenberth and Stepaniak 2001: Wang and Fiedler 2006). SSTs that are anomalously low (<-0.5 degrees °C) are classified as a La Niña pattern, whereas anomalously high SSTs (> 0.5 degrees °C) are classified as an El Niño. Both patterns are responsible for impacting precipitation anomalies in the United States through tropical-extratropical teleconnections that alter the jet stream and storm track (Power et al. 2013; Du et al. 2020; Kim et al. 2021). During an El Niño, the subtropical jet stream is located across the southern United States, bringing wetter winters to the south and drier winters to the north (Du et al. 2020; Kim et al. 2021). In a La Niña, the effects are that the subtropical jet stream becomes more variable, moving across the northern United States, resulting in wetter winters to the north and drier winters to the south.

On subseasonal timescales (weeks to months) certain large-scale flow patterns appear continuously at fixed geographical locations and persist beyond the lifetimes of individual weather disturbances in the mid-latitudes, on average for about 14 days and up to 30 days (Robertson et al. 2020). This concept is known as weather regimes (Reinhold and Pierrehumbert 1982; Cassou et al. 2004). Similarly, jet regimes relate to the characteristics of the North Pacific Jet and North Atlantic Jet (Winters and Walker 2022). Unlike weather regimes, jet regimes focus on the state and evolution of these jets and associate them with an increased likelihood for winter storms (Winters and Walker 2022). Weather regimes encompass broader atmospheric patterns and conditions (Robertson et al. 2020). There are four defined North American weather-regimes that strongly impact precipitation and temperatures, including extreme flooding and precipitation-type across the US (Robertson et al. 2020). They are defined by the most prominent geopotential height anomalies. There are currently no studies that link seasonal to interannual ENSO precipitation variability or subseasonal precipitation variability associated with weather regimes to vehicle crashes. The goal of this study is to investigate the following connections throughout the continental United States (CONUS): ENSO->precipitation variability->fatal crashes for the seasonal to interannual timescale and weather regimes->precipitation variability->fatal crashes for the subseasonal timescale (Figure 1). A macro-scale approach is adopted, which considers both temporal and spatial weather-related crash analysis (Perrels et al. 2015). This requires consideration of car crashes that have occurred nationwide with time. This differs from a micro-scale approach in that the latter considers spatial patterns alone and draws focus on specific weather events and regions (Perrels et al. 2015).

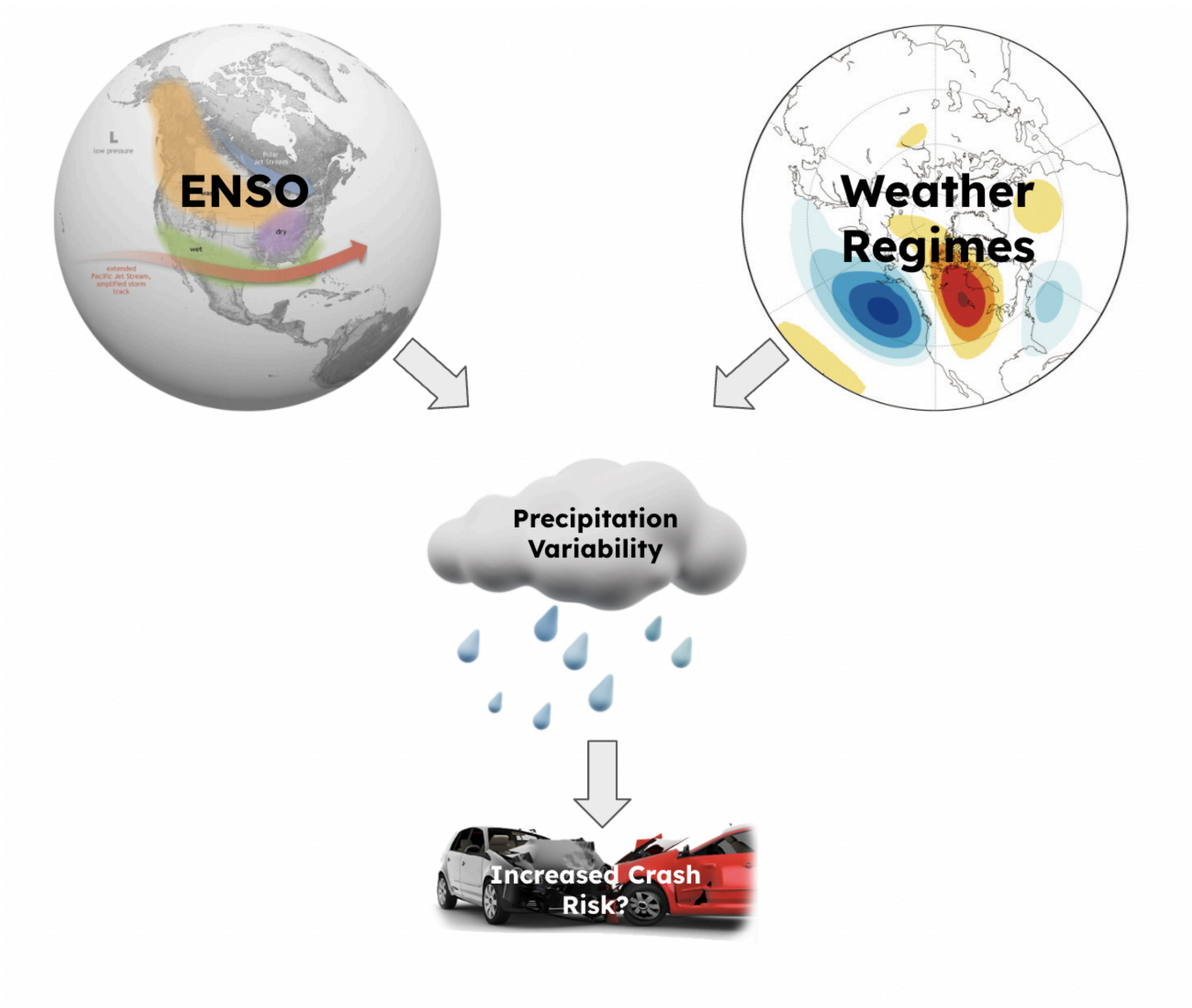

Figure 1. Possible connections of ENSO and Weather-Regimes to occurrence of vehicle-crashes.

CHAPTER 2: DATA AND METHODS

2.1 Region Definitions

This study is focused on all 50 states for demonstrating relationships between the Niño 3.4 index and fatal weather-related crashes over time. States are also aggregated into five major geographic regions to summarize regional impacts of ENSO or weather regimes on fatal weather-related crash anomalies (FWRCA). The regions used are: the West Coast, the Mountain West, the North Central, the South, and the Northeast (Figure 2).

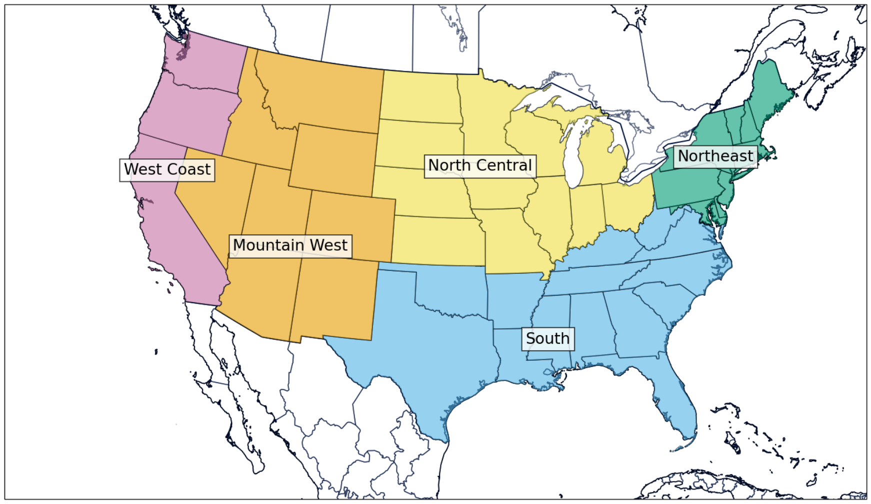

Figure 2. Map of the United States showing five major geographic regions: West Coast (purple), Mountain West (orange), North Central (yellow), South (blue), and Northeast (teal). The map excludes Alaska, Hawaii, and U.S. territories.

2.2 Seasonal Definitions

In the United States, the following four seasons are defined based on their differing temperature and weather patterns: (1) Fall, (2) Winter, (3) Spring, and (4) Summer. Out of the four seasons, the Winter season (consisting of December, January, and February) typically has not only the most liquid and frozen precipitation fallen, but is also a period where ENSO impacts are the strongest. Therefore, the analysis is done during this season.

2.3 Data

2.3.1 Fatal Analysis Reporting System data

To analyze fatal motor vehicle crashes, this study uses the Fatal Analysis Reporting System (FARS) data (NHTSA 2025). The FARS data is the most comprehensive dataset for fatal vehicle crash data in the United States. This dataset documents vehicle crashes that resulted in a fatality within 30 days of a crash occurring through medical, vital, and police reports for all 50 states, Washington D.C., and Puerto Rico (Wilson and Stimpson 2010; Yan et al. 2020; NHTSA

2025). In this study, FARS data was extracted from 1981-2019 and filtered to only include the December, January, and February months (DJF). Additionally, the data was filtered to only include crash fatalities that occurred during some form of adverse weather (Figure 3). This included both precipitation-related and non-precipitation related weather types. The “Other” and “Unknown” weather-related fatalities were excluded due to the uncertainty of the weather type involved.

Fatal crashes vary widely by state due to factors including population, driving habits, state-specific policies, and climatology. This is also to explore the general crash trends from before the introduction of the coronavirus outbreak after 2019. Normalized anomalies of the total weather-related crash fatalities are used to account for this variability. They are calculated by subtracting out the mean fatal weather-related crashes over all years for a given month and state. Then, the value is normalized by the standard deviation, creating a variable called the FWRCA.

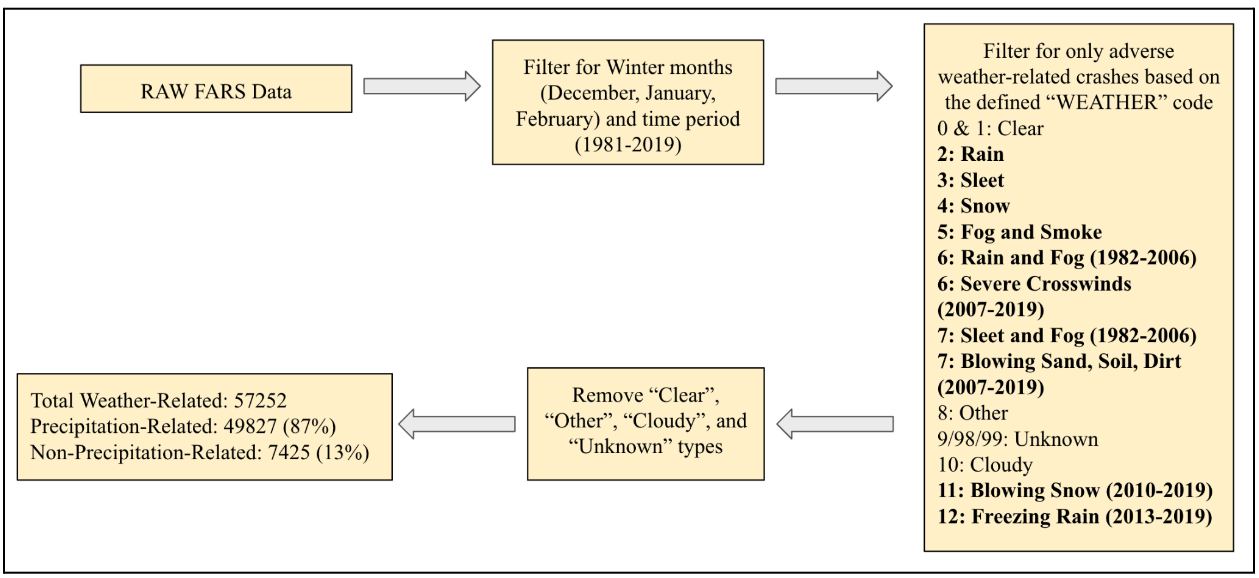

Figure 3. Steps of the crash filtering process.

2.3.2 El Nino-Southern Oscillation Index and Data

Since it is known that precipitation variability is driven by ENSO, this work uses the Niño 3.4 index to represent the average equatorial sea surface temperature anomalies in the tropical Pacific (Bunge and Clarke 2008;Yu and Kim 2013; Kostis 2019). This allows ENSO events to be identified. This index comes from the National Oceanic and Atmospheric

Administration (NOAA) Physical Sciences Laboratory (Huang et al. 2017). These anomalies are calculated by taking the difference of the actual monthly SST value and the mean SSt value, averaged over the region ranging from 5°N-5°S latitude and 170-120°W longitude (Huang et al. 2017). This data is then normalized by dividing the SST anomalies by its standard deviation. Each monthly period exceeding an SST anomaly of 0.5 °C above normal is documented as an El Niño year. For each anomalously low period (SST of -0.5 °C below normal or less), this is considered a La Niña year.

To confirm the direct effects of ENSO on transportation and road safety, the historical cold and warm ENSO episodes have been extracted to identify cases of a La Niña or an El Niño by year using the Niño 3.4 index. Although SST anomaly data has been available since 1870, this study focuses on the time period from 1981-2019 to match the time period used for FARS (Figure 4). The majority of the analysis also looked into the effects of ENSO teleconnections during the DJF season since its impacts are the most prominent during this season (Mo and Schemm 2008).

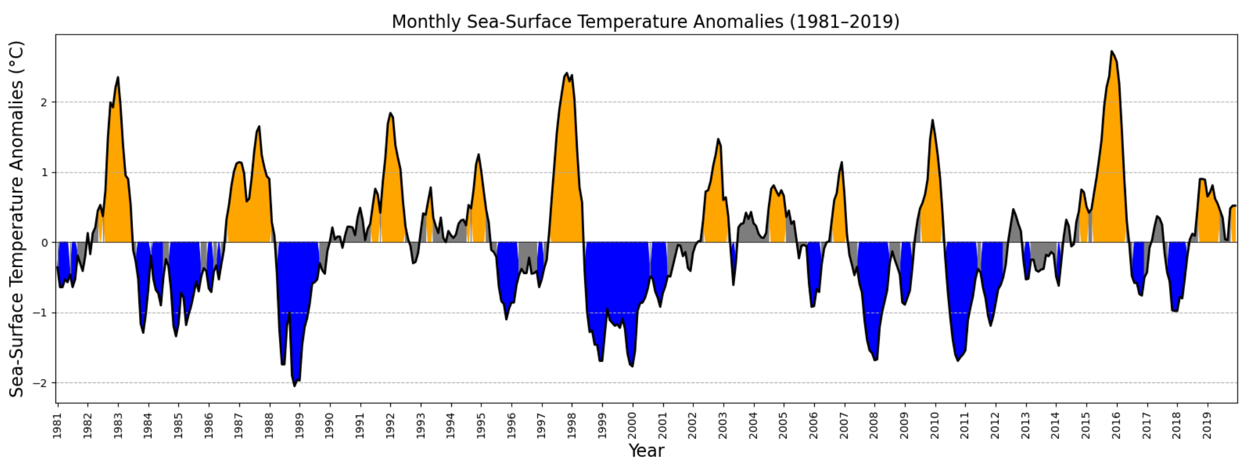

Figure 4. Time Series of the Niño 3.4. index highlighting periods of below and above normal SSTs from January 1981-December 2019. Documented El Niño (La Niña) anomalies are colored in orange (blue) when the SST anomaly threshold is succeeded.

The fatal weather-related crash anomalies are shown in Figure 5. Twelve line values were plotted for each year, with one line value plotted per month. In some years, peak crashes follow a strong El Niño (Figures 4 and 5). FWRCA peaks at the beginning and end of most years. One important thing to highlight is that the FWRCA values have declined over time, as shown by the progressively negative monthly anomalies in recent years. There are also instances where an offset occurs between FWRCA and SST anomalies.

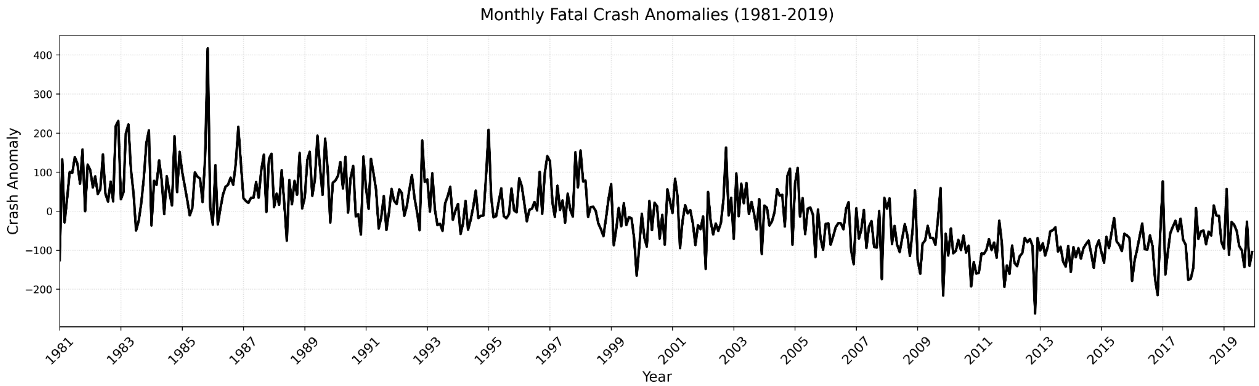

Figure 5. Monthly fatal weather-related crash anomalies by year for all months (1981-2019).

2.3.3 Precipitation Data

The precipitation data used is the 0.05° Climate Hazards Group InfraRed Precipitation with Station data (CHIRPS) v2 dataset. It is a quasi-global (50°S - 50°N) land-only rainfall dataset available from 1981-present years (Funk et al. 2015). To account for differences in precipitation climatology across the US, precipitation anomalies are used.

Precipitation variability due to ENSO (Seager et al. 2005) and weather regimes (Amini and Straus 2019; Lee et al. 2020; Molina et al. 2023) across the US is well known. Since transportation in the US is managed by state departments of transportation (DoTs), precipitation variability is investigated by state. The average precipitation anomalies are calculated for each state from the CHIRPS data using state shape files from the United States Census Bureau (2024). Figures 6 and 7 show the average precipitation anomalies for El Niño and La Niña events by state, respectively. Values were shown to be the most variable for states in the south, consistent with the knowledge that winters in the south are wetter than normal during an El Niño and drier than normal during a La Niña (Schmidt et al. 2001; Schmidt and Luther 2002).Every state in the Southern region contained positive and negative precipitation anomalies during an El Niño and a La Niña period, respectively. The same difference is also prevalent in the Mountain West region, though the precipitation anomalies were relatively weaker.

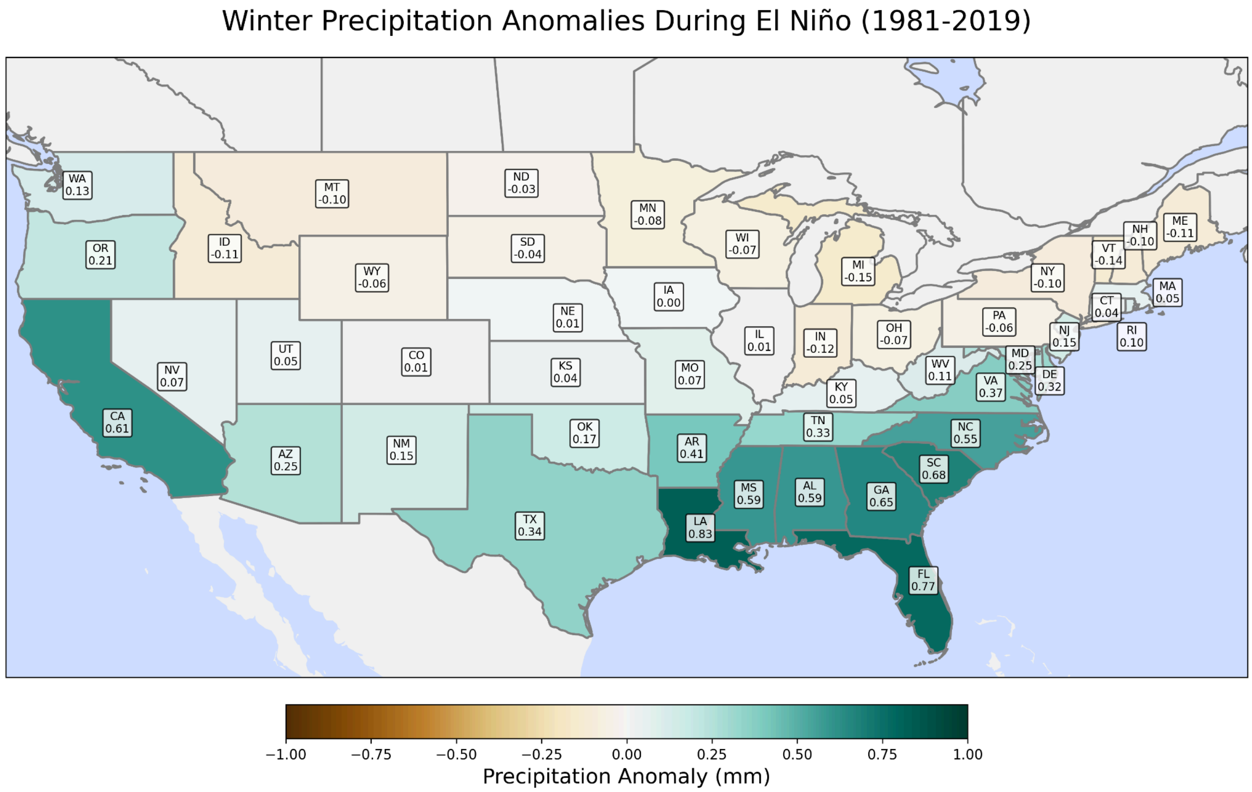

Figure 6. Map of the winter precipitation anomalies during the DJF season for each state in CONUS during an El Niño.

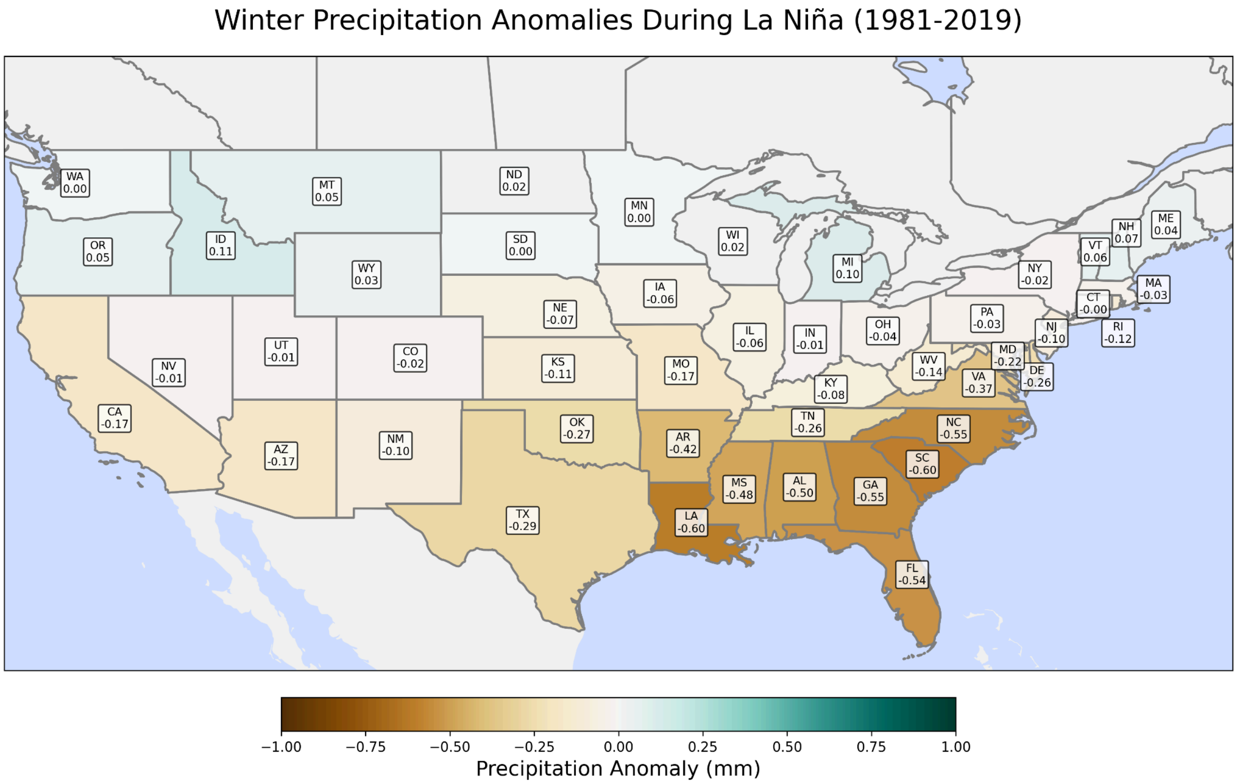

Figure 7. Map of the winter precipitation anomalies during the DJF season for each state in CONUS during a La Niña.

2.3.4 Snow Water Equivalent Data

One limitation of the CHIRPS dataset is that while it provides high resolution precipitation anomalies, the values represent all forms of precipitation rather than specific types of precipitation. During the winter, frozen precipitation is much more prevalent in the United States. Because frozen precipitation impacts traffic conditions (Datla and Sharma 2008; Kwon et al. 2013; Roh et al. 2013), snow water equivalent (SWE) data is used to identify how much precipitation is in the form of snow or other frozen precipitation (such as sleet). SWE quantifies the amount of liquid water in the snow pack that would be formed if the snowpack were to be completely melted (Luojus et al. 2021). SWE data is obtained from the National Snow and Ice Data Center (NSIDC) via the National Operational Hydrologic Remote Sensing Center (NOHRSC) data archive (NOHRSC 2004). It is available for 2003-present at a 1 km spatial resolution (NOHRSC 2004). Unlike the FARS, precipitation, and ENSO Data, SWE information from prior to 2003 is not available. While this is a caveat, the period from 2003-2019 can still be analyzed with the other datasets that this work uses. The anomalies of SWE are calculated to account for variability in climatology of snow and frozen precipitation. The snow water equivalent anomalies (SWEA) are averaged for each state using the US Census Bureau (2024) state shape files. Based on the quality control documentation provided by NSIDC, all SWE values ≥ 32.767m are set to 32.767m (NOHRSC 2004). Figures 8 and 9 show the average SWE anomalies for each state during El Niño and La Niña. The most positive and negative values are generally found in the North East and North parts of the West Coast and Mountain West during La Niña and El Niño years, respectively. This differs from Figures 6 and 7 where precipitation anomaly extremes were mainly concentrated in the south.

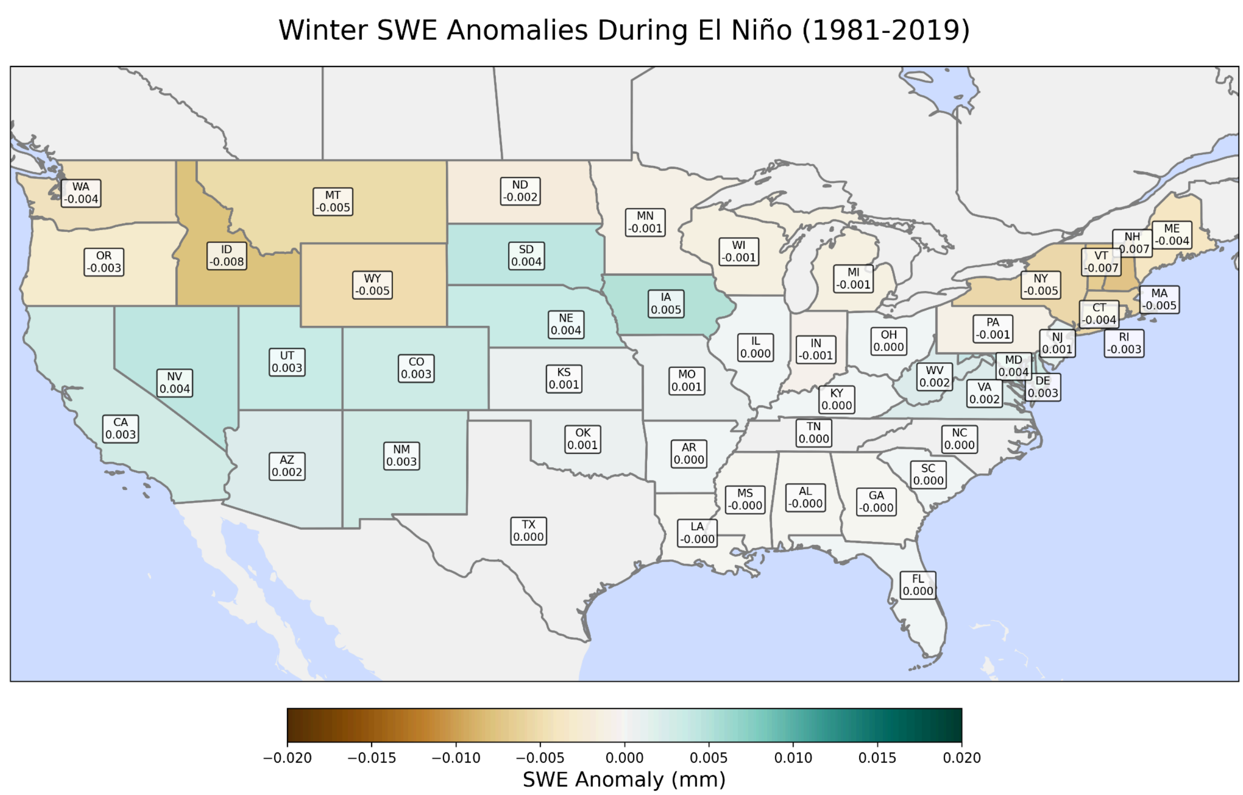

Figure 8. Map of the winter SWE anomalies during the DJF season for each state in CONUS during an El Niño period.

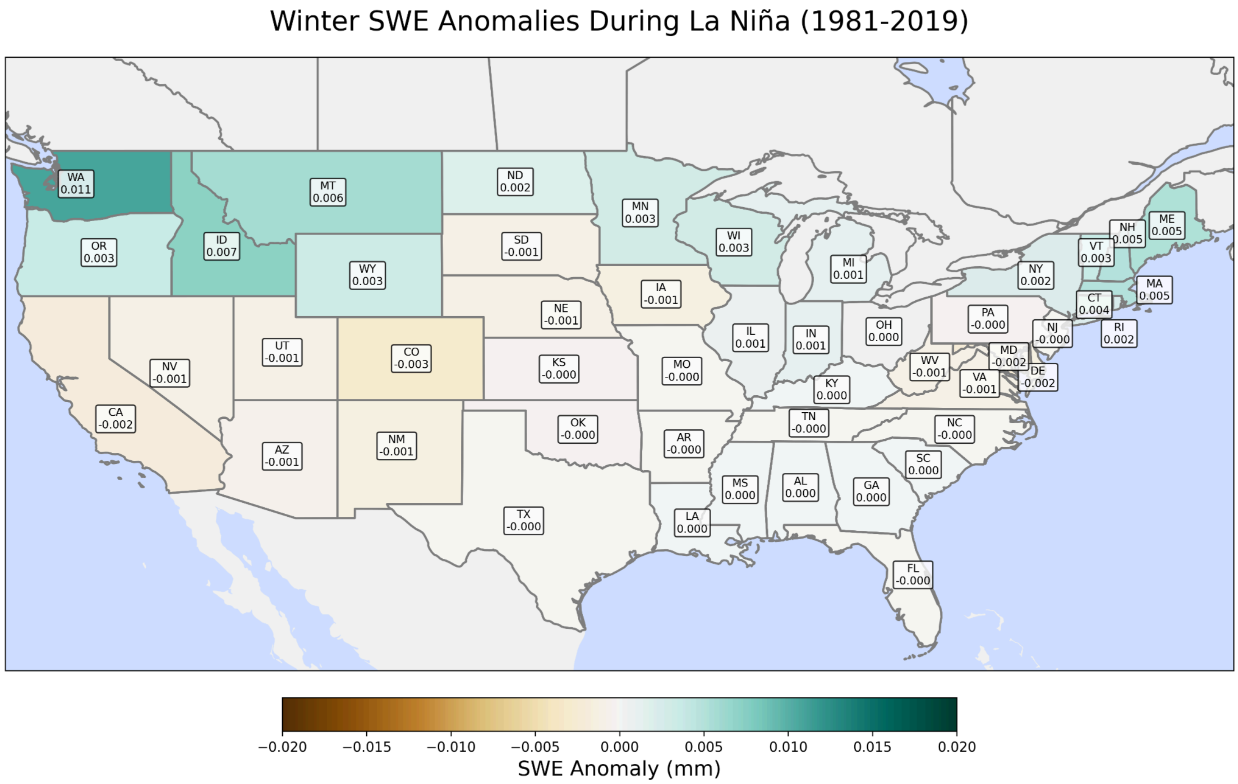

Figure 9. Map of the winter SWE anomalies during the DJF season for each state in CONUS during a La Niña period.

2.3.5 Weather Regimes

Regional precipitation variability can be further understood by looking at how precipitation patterns vary for persistent large scale atmospheric phenomena known as weather regimes. Using k-means clustering, four North American weather regimes were identified from the 500hPa geopotential height (Z500) anomalies using the European Center for Medium Range Weather Forecast, 5th generation reanalysis (Hersbach et al. 2020), following Molina et al. (2023): The Alaskan Ridge (Pacific Ridge), The Greenland High, The Pacific Trough, and The West Coast Trough (Figure 10). The most prevalent regime is the Pacific Trough, with a frequency of 29% . Since these regimes can be persistent for a long period of time (Francis et al. 2018), they can impact regional precipitation anomalies (Figure 11).

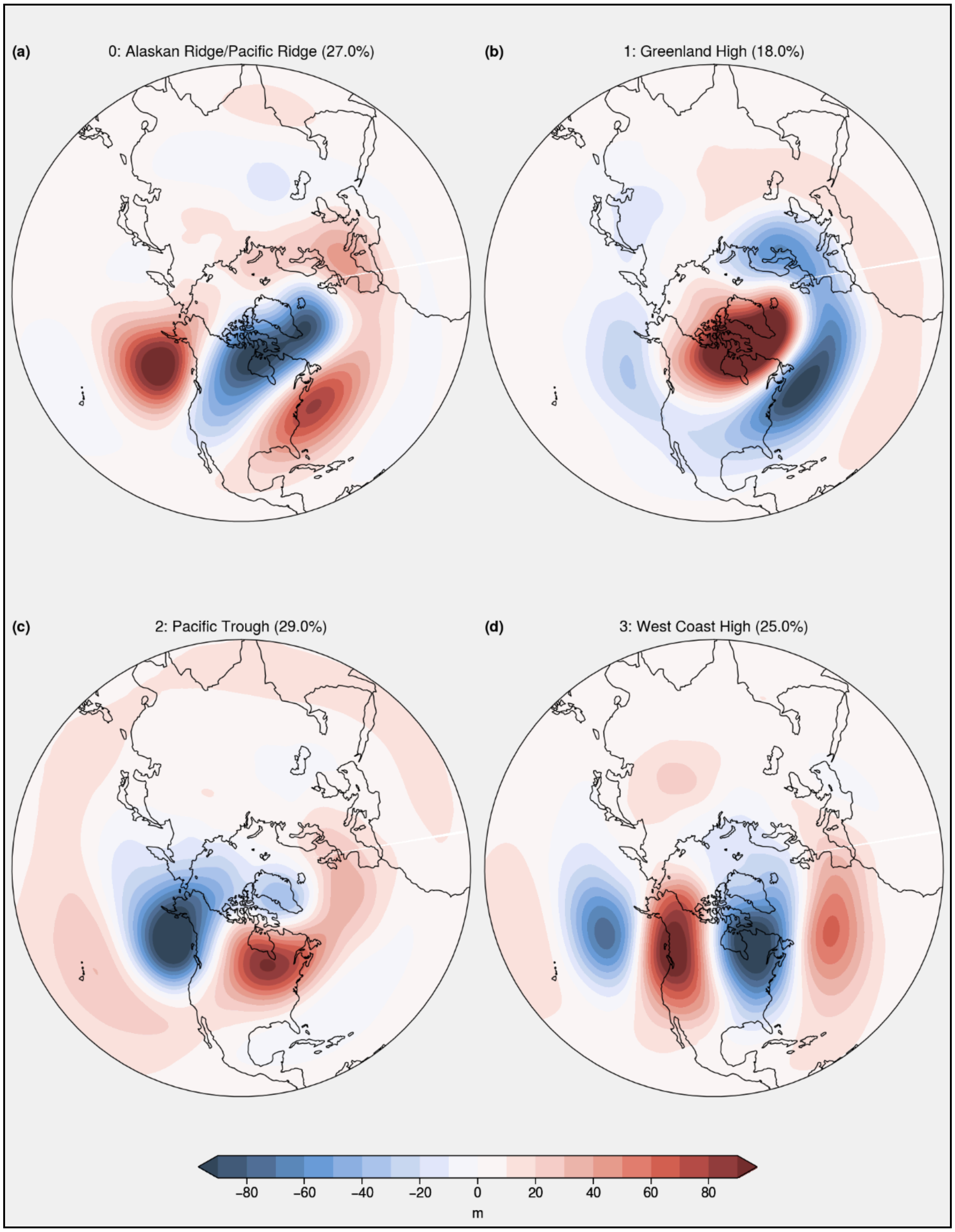

Figure 10. Composite Z500 anomalies for each of the four regimes: (a) Alaskan/Pacific Ridge, (b) Greenland High, (c) Pacific Trough, and (d) West Coast High.

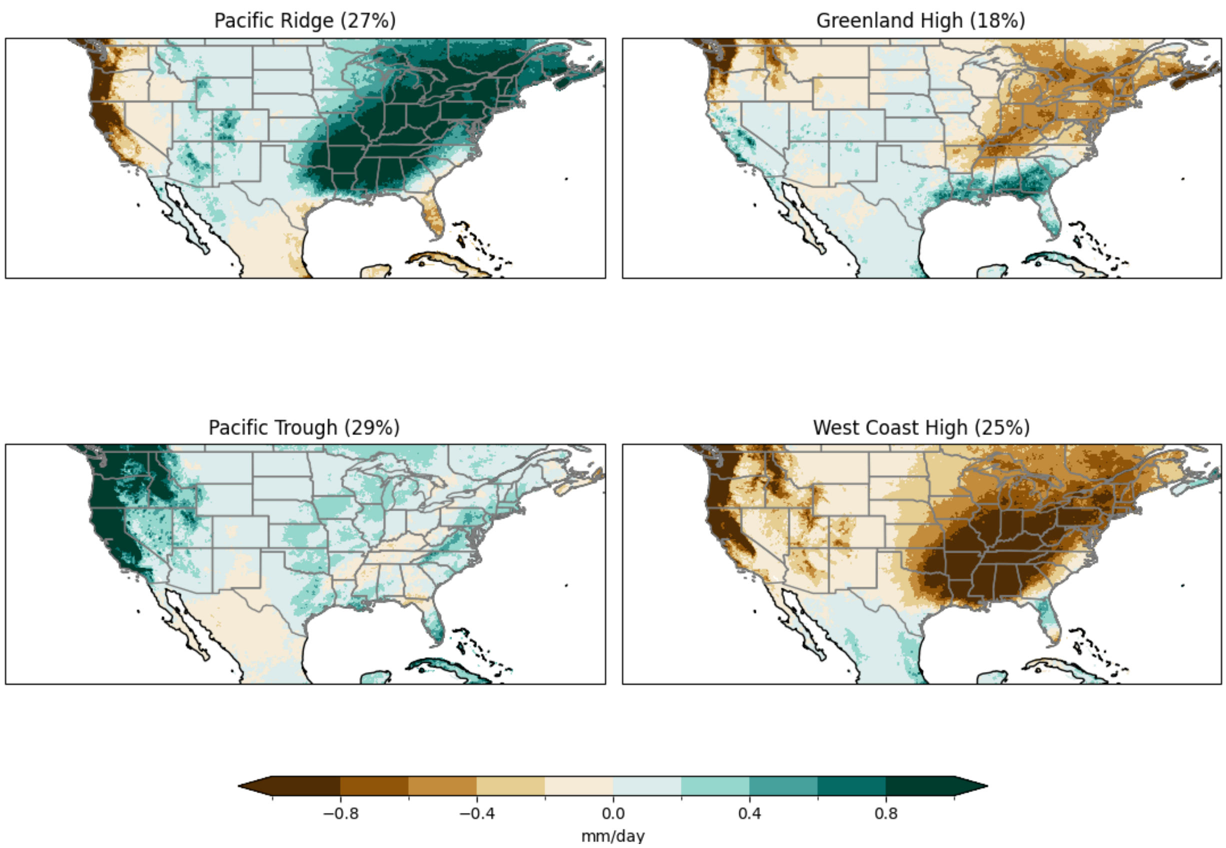

Figure 11. Map of the composite precipitation anomaly distribution for the continental United States for each defined regime: Pacific Ridge, Greenland High, Pacific Trough, and the West Coast High. Values in green indicate positive precipitation anomalies, while values in b indicate negative precipitation anomalies [adapted from Lee et al. 2023].

2.4 Methods

2.4.1 Linear Regression

The linear relationship between fatal weather-related crash anomalies and precipitation anomalies is identified using linear regression as follows:

$$FWRCA = aP + b \qquad (1)$$

Where *FWRCA* is the fatal weather-related crash anomaly., *P* is the precipitation anomaly, *a* is the slope, and *b* is the y-intercept. The variance explained (R^2) by the regression line indicates a measure of the linear relationship between precipitation anomalies and FWRCA.

2.4.2 ENSO-related vs Non-ENSO-related Precipitation Data

This study investigates precipitation variability due to ENSO. However, precipitation variability may come from many sources other than ENSO. Therefore, it is separated into its ENSO and non-ENSO components using linear regression. Assuming that non-linear interactions are not considered, the total precipitation anomaly can be separated into its ENSO and non-ENSO components as follows:

$$P_{tot} = P_{ENSO} + P_{NON\text{-}ENSO} \qquad (2)$$

where *P(tot)* is the total precipitation anomaly, *P(ENSO)* is all precipitation anomalies linearly related to ENSO-, and *P(NON-ENSO)* is all precipitation anomalies not linearly related to ENSO.

The ENSO-related precipitation anomalies can be identified by linear regression between the Nino3.4 index and the total precipitation anomalies. The resulting precipitation is the ENSO-related precipitation, as follows:

$$P_{ENSO} = a(N3.4) + b \qquad (3)$$

where *N3.4* are the SST anomalies from the Niño 3.4 index. The non-ENSO related precipitation anomalies can then be calculated by taking the difference of P(ENSO) and P(tot).

2.4.3 Weather Regime Analysis

In a given month, a certain regime dominates. This means that precipitation patterns will skew towards the dominant regime at a given time. In Figure 11, precipitation anomalies vary regionally from regime to regime. These precipitation composite plots provide a good indication of where precipitation dominates. For example, the changes in precipitation anomalies were constantly marginal in the Mountain West for each regime. This helps filter down the states and regions where mean precipitation anomalies are more positive or negative.

For each region and for each state, the focus is to find the relationship between different weather regimes and fatal weather-related crashes. This includes normalizing the regime-crash relationship by the average crashes per day for each regime, because each regime happens at a different frequency. Moreover, the same analysis is done again accounting for the percentage of crashes that occur for each regime in each region. This is repeated again but for individual states. The percentages can confirm the dominant regime that was diagnosed based on the average crashes per day.

CHAPTER 3: RESULTS

3.1 Relationship between FWRCA and total precipitation anomalies

To understand which states are most affected by precipitation, the linear relationship between total precipitation anomalies and FWRCA is shown in Figure 12. The top six states where precipitation anomalies impact FWRCA are: California, Arizona, Nevada, Oregon, Texas, and Georgia. The largest variance of FWRCA explained by total precipitation anomalies occurs for California (48%) and Arizona (45%). Four of the top six states experience positive precipitation anomalies during an El Niño and negative precipitation anomalies during a La Niña: California, Arizona, Georgia, and Texas (Figures 6 and 7). This is consistent with previous work showing these states are impacted by ENSO (Hansen et al. 1998; Du et al. 2020).

The majority of states with a stronger relationship between FWRCA and total precipitation anomalies, as indicated by the R^2 value, were in the low latitudes (Figure 12). There is a stronger relationship across the southern US between precipitation anomalies and FWRCA. States that are located in the Northeast and North Central regions showed the weakest relationship between total precipitation anomalies and FWRCA, while the relationships were mixed in the Mountain West.

The statistical significance of the relationship between total precipitation anomalies and FWRCA is highlighted in Figure 13. This was done by taking a sample size of 39 years worth of data to find the minimum R^2 required for the value to be statistically different from zero ($p < 0.05$). With a threshold of 10%, all states in the West Coast, as well as some in the Southern, North Central, and Mountain West regions, held R^2 values that were significantly different from zero. To contrast, the northern parts of the Mountain West, North Central, and all of the Northeast had R^2 values that were not statistically different from zero.

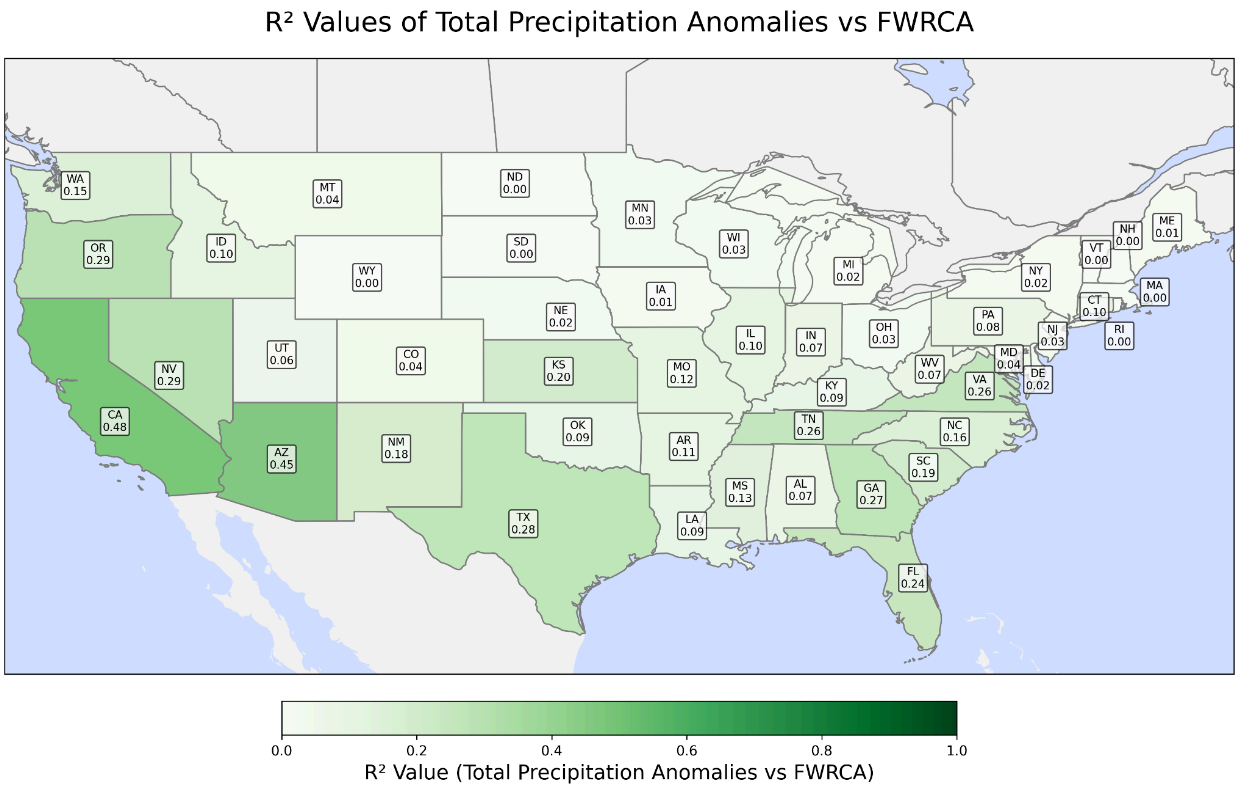

Figure 12. Map of the R^2 values of the Total Precipitation Anomalies vs FWRCA during the DJF season for each state in CONUS.

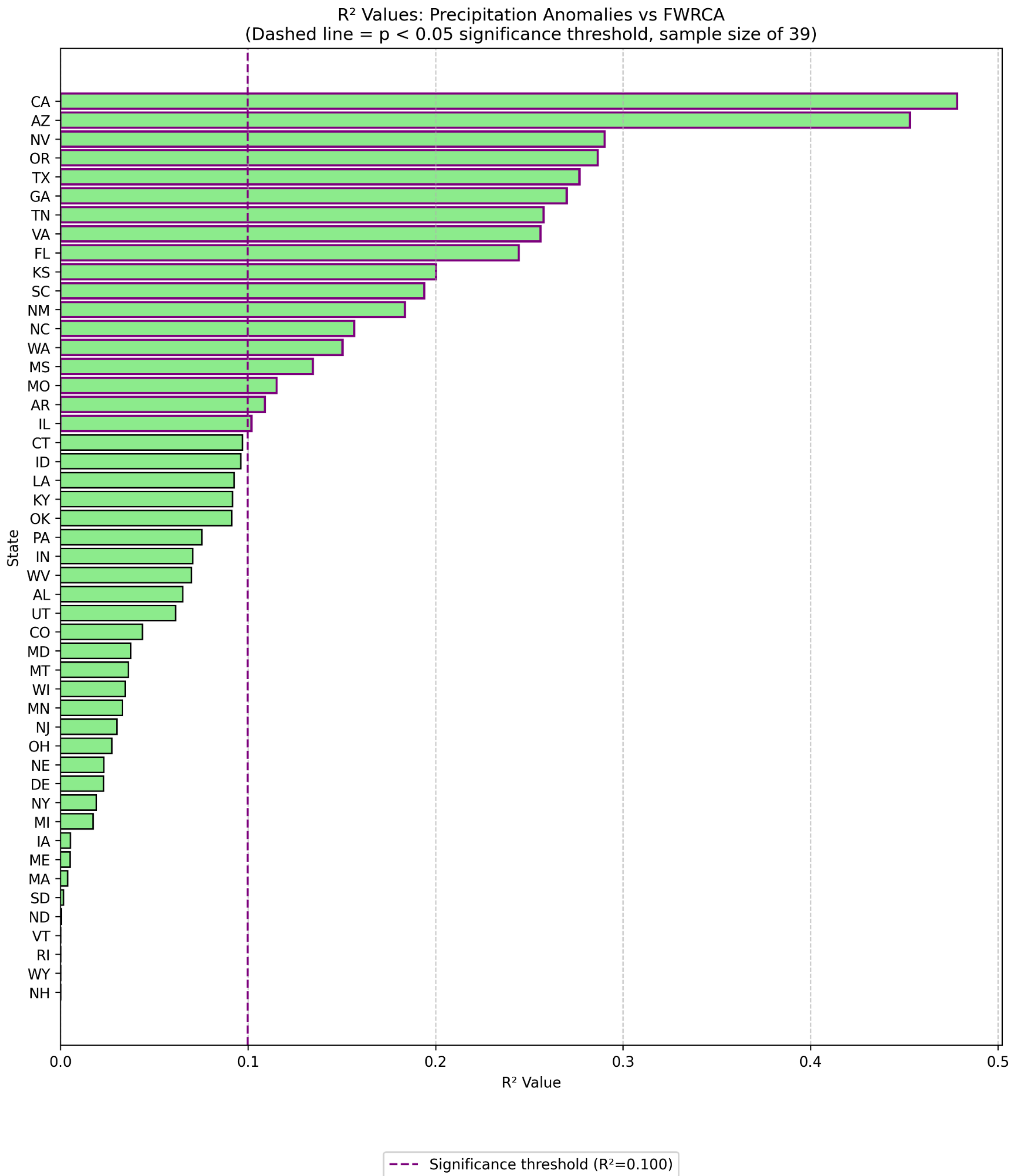

Figure 13. Barplot of the R^2 values of the Total Precipitation Anomalies vs FWRCA during the DJF season for each state in CONUS, with the significance threshold highlighted in purple.

Snow events can lead to impacts that can last for days or even weeks. Since snow creates hazardous road conditions, snow water equivalent anomalies (SWEA) are used to identify how much of the precipitation of snow and frozen precipitation and investigate the relationship between winter precipitation and fatal weather-related crash anomalies (Figure 14). California had the strongest relationship, with 36% of the variance explained by SWEA. However, this relationship is relatively weak for every other state in CONUS. This suggests that snowfall and frozen precipitation is a large contributor to the relationship between precipitation variability and FWRCA in California, while contributing little to none in other states.

The statistical significance between SWEA and FWRCA is presented in Figure 15. Since the SWE data only goes back to 2003, a sample size of 17 years was used. The significance threshold was found to be more than twice as high as the threshold for precipitation and FWRCA at the 5% level. With a threshold of 23.2%, California is the only state that had a statistically different relationship from zero between SWEA and FWRCA.

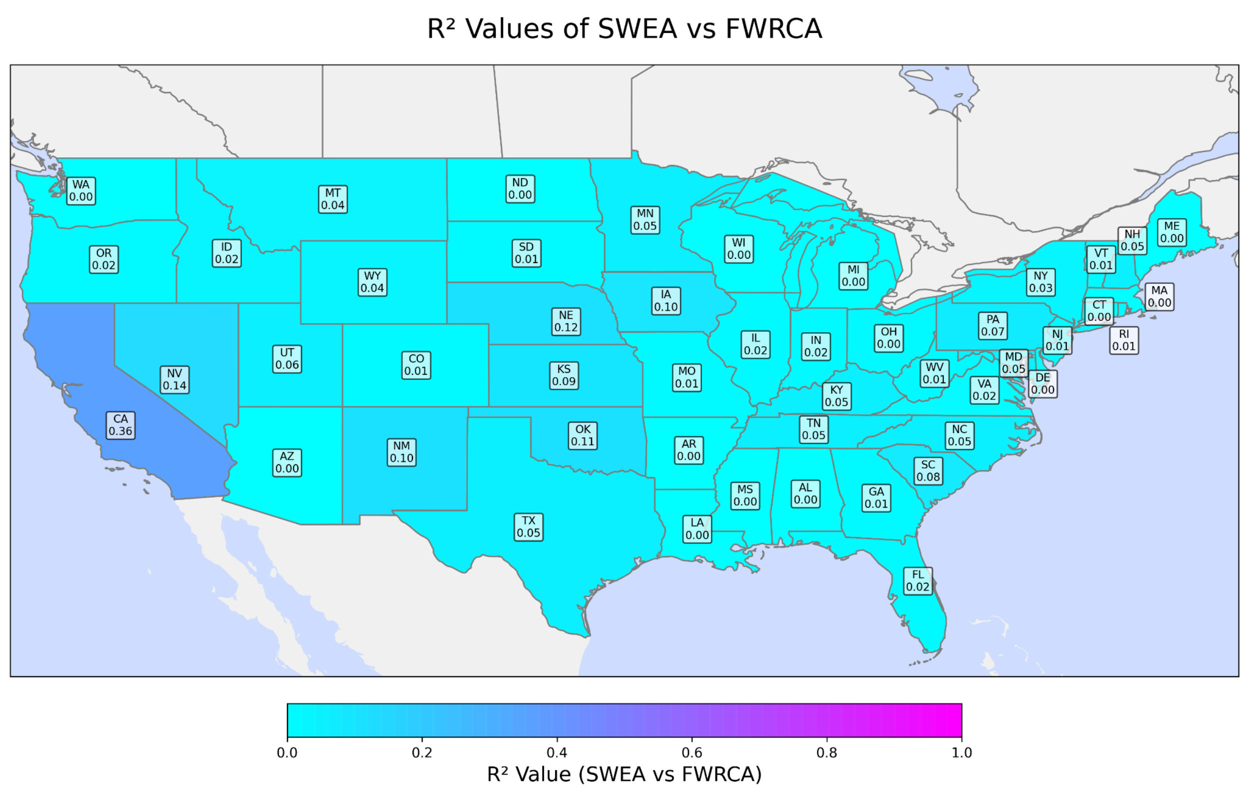

Figure 14. Map of the R^2 values of SWEA vs FWRCA during the DJF season (Both Normalized) for each state in CONUS.

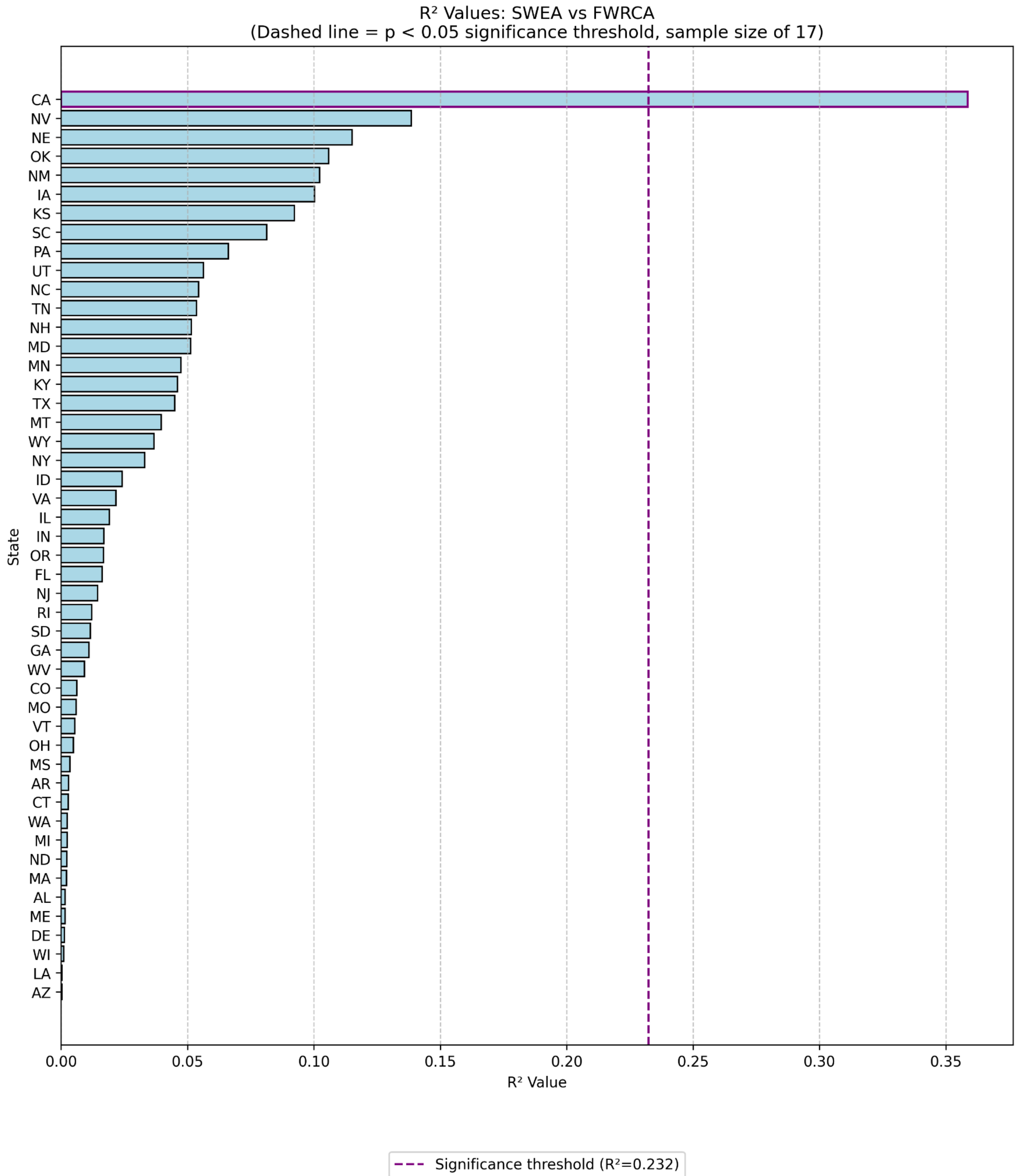

Figure 15. Barplot of the R^2 values of the SWEA vs FWRCA during the DJF season for each state in CONUS, with the significance threshold highlighted in purple.

3.2 Relationship between ENSO-related precipitation anomalies and FWRCA

To determine how FWRCA are related to ENSO-related precipitation anomalies, the linear relationship between them for each state is shown in Figure 16. Despite the fact that ENSO impacts precipitation anomalies for most states (Figure 6 and 7), FWRCA is less sensitive to ENSO-related precipitation anomalies. Even in California, a state known for being impacted by ENSO, less than 1% of the FWRCA variance is explained by precipitation anomalies (Figure 16).

Temperature and precipitation variability associated with ENSO can potentially impact whether precipitation falls as snow or liquid (Patten et al. 2003). The relationship between ENSO-related SWEA and FWRCA is presented in Figure 17. Unlike the relationship with the total SWEA, the relationships were relatively weak throughout the United States. The strongest ENSO-related SWEA vs FWRCA relationship was in Virginia (~20%), which is not a large enough $R^2$for this relationship to be statistically significant.

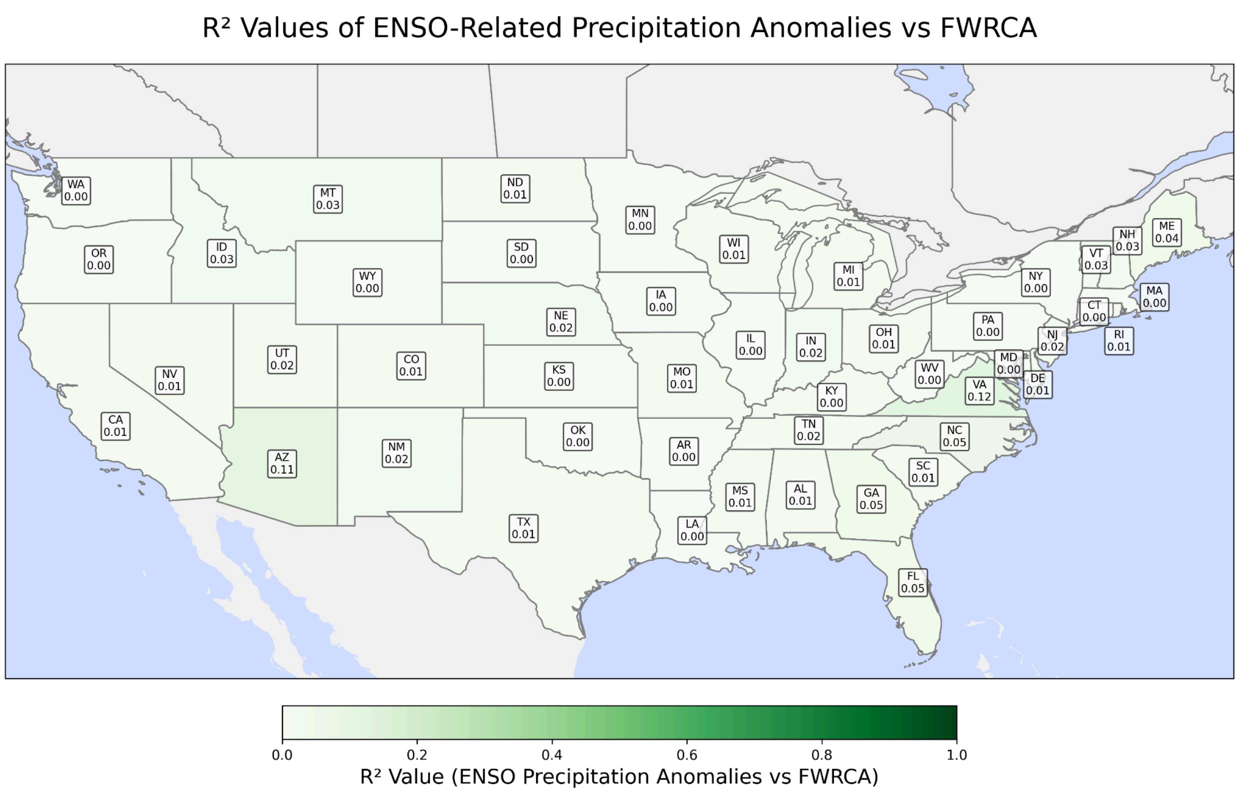

Figure 16. Map of the R^2 values of the ENSO-related Precipitation Anomalies vs FWRCA during the DJF season (Both Normalized) for each state in CONUS.

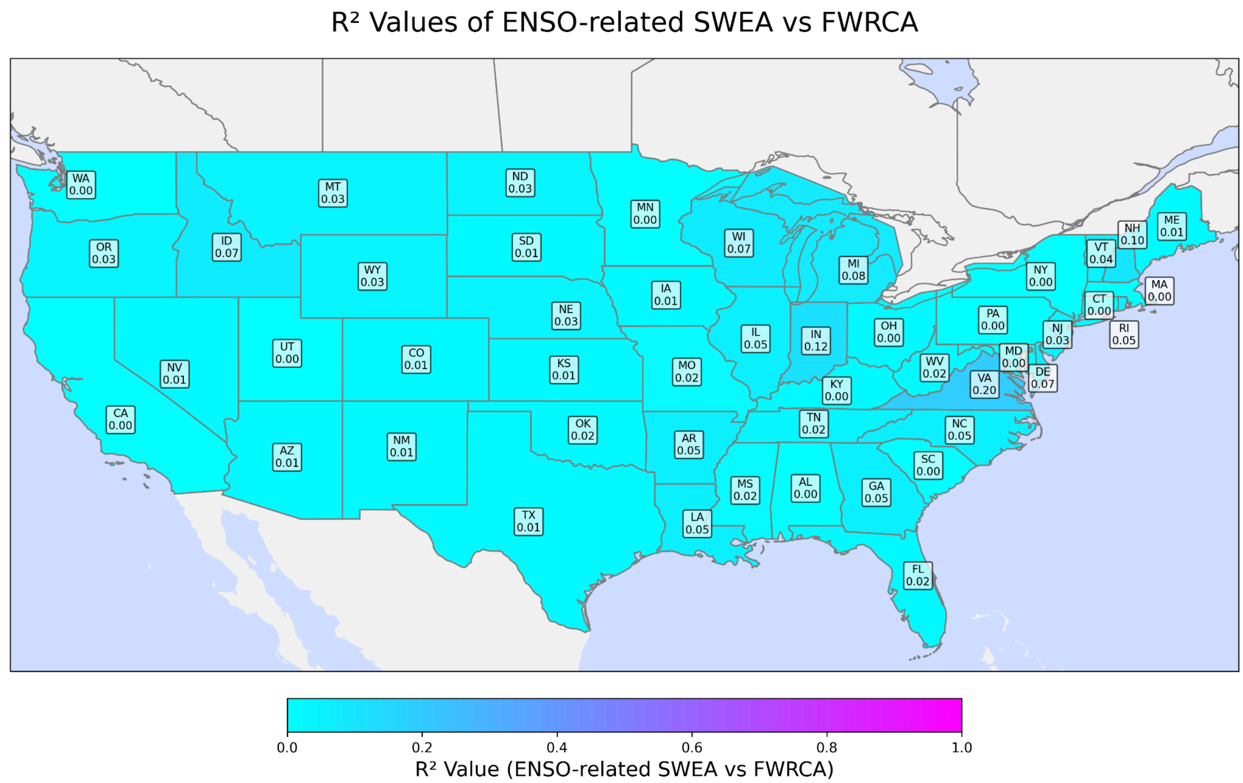

Figure 17. Map of the R^2 values of the ENSO-related SWEA vs FWRCA during the DJF season (Both Normalized) for each state.

3.3 Relationship between weather-regimes related precipitation anomalies and FWRCA

3.3.1 Precipitation Anomaly Distribution for Each Regime

There are several differences in the composite anomalies for each regime. The majority of the eastern parts of the North Central, the Northeast, and the Southern United States show anomalously high and low precipitation anomalies during periods of the Pacific Ridge and West Coast High, respectively. Positive precipitation anomalies in the West Coast are associated with The Pacific Trough while negative anomalies occur during the Pacific Ridge and West Coast High. The Mountain West and the western portion of the North Central show little difference in precipitation anomalies regardless of the regime (Figure 11). The Greenland High impacts the overall United States precipitation variability the least, with the largest anomaly magnitudes occurring in the West Coast as well as the Florida panhandle.

3.3.2 Fatal Crash Frequency by Weather Regime

The frequency of fatal crashes is investigated for each weather regime for CONUS as a whole and for each region. The number of days that are associated with each regime is shown in Table 1. Since there is variability in the number of days each regime occurs (Table 1), comparison of crashes between regimes is performed by first dividing the total number of weather-related crashes by the number of days in each regime and calculating the average number of crashes per day in each regime (Figure 18). The Pacific Ridge has the highest crash frequency with ~18 crashes per day over all of CONUS, followed by the Greenland High and Pacific Trough with ~16 crashes per day each. The least amount of crashes per day occurred during a West Coast High regime, where only an average of ~14 crashes per day was found. The confidence intervals help indicate where the mean crashes per day could fall. In order to determine if there are non-random differences in crashes per day for each regime, a sample size was determined based on the numbers of daily values during the winters of 1981-2019 for each regime. This number has been divided by 28 days (4 weeks) to check for confidence. This sample size is different for every regime as their frequencies vary (Table 1). From here, a t-test was used with an alpha (level of significance) at 5%. The average crashes per day for the Pacific Ridge and West Coast High are statistically different from the averages crashes per day in the other defined weather regimes. This is explained from the confidence intervals not overlapping with each other. Moreover, the average number of crashes per day during the Greenland High and Pacific Trough regimes remain fairly similar to each other.

Table 1. Number of days that each regime (Pacific Ridge, Greenland High, Pacific Trough, and West Coast High) dominates over a period of 1981-2019.

Regime Name	Number of days in each regime
Pacific Ridge	1004
Greenland High	611
Pacific Trough	995
West Coast High	909

Despite the Pacific Ridge having the highest number of crashes per day over all of CONUS, this is not the case for every region in the United States. In the West Coast, the Pacific Trough has the highest average crashes per day (Figure 19). Most regions experience the highest average crashes per day during the Pacific Ridge (Figures 19). In the West Coast, however, the Pacific Trough has the highest average crashes per day (Figure 19). The average crashes per day were consistently the lowest during the West Coast High for every region (Figure 19). In the South, there is no overlap of the confidence intervals when comparing the average crashes per day during a Pacific Ridge to the West Coast High. This indicates that the average crashes per day during a Pacific Ridge for the South is significantly different than that of the West Coast High. In the North Central, Mountain West, and West Coast regions, the intervals overlap, so the average crashes per day per regime is not significantly different from one another. In the Northeast, there is some overlapping between the intervals from each regime, which also indicates a lack of significance.

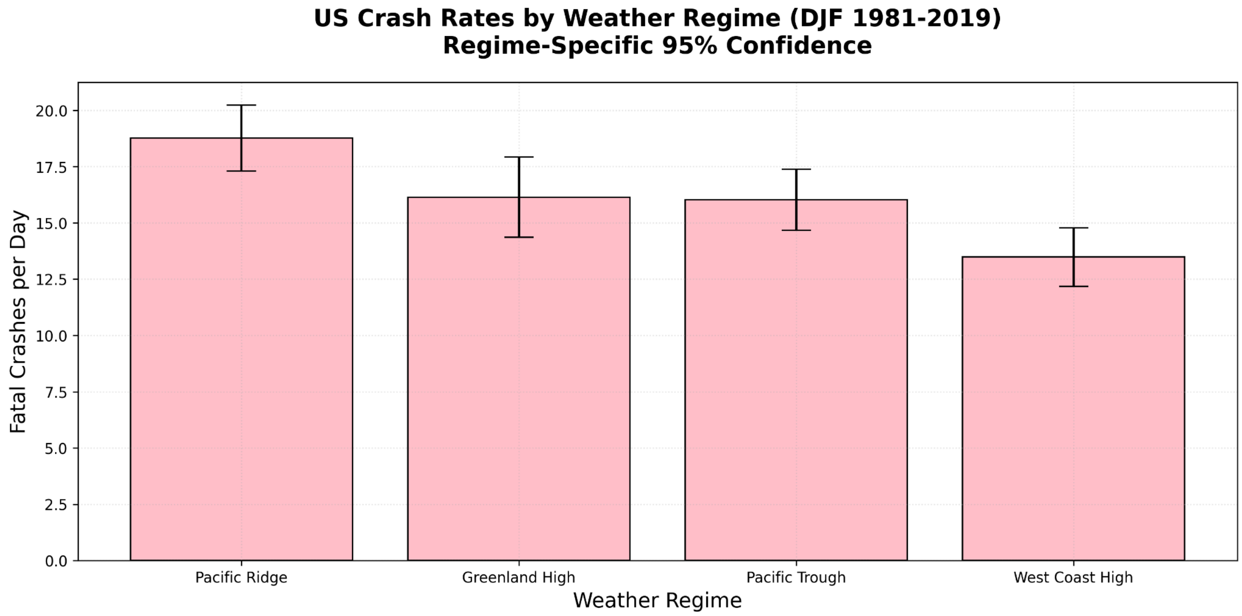

Figure 18. Barplot of the Fatal Crash Rate by Weather Regime for all of the Contiguous US. The Weather Regime type is shown on the x-axis and the crashes per day are shown on the y-axis. The 95% confidence interval is shown on the top of each bar.

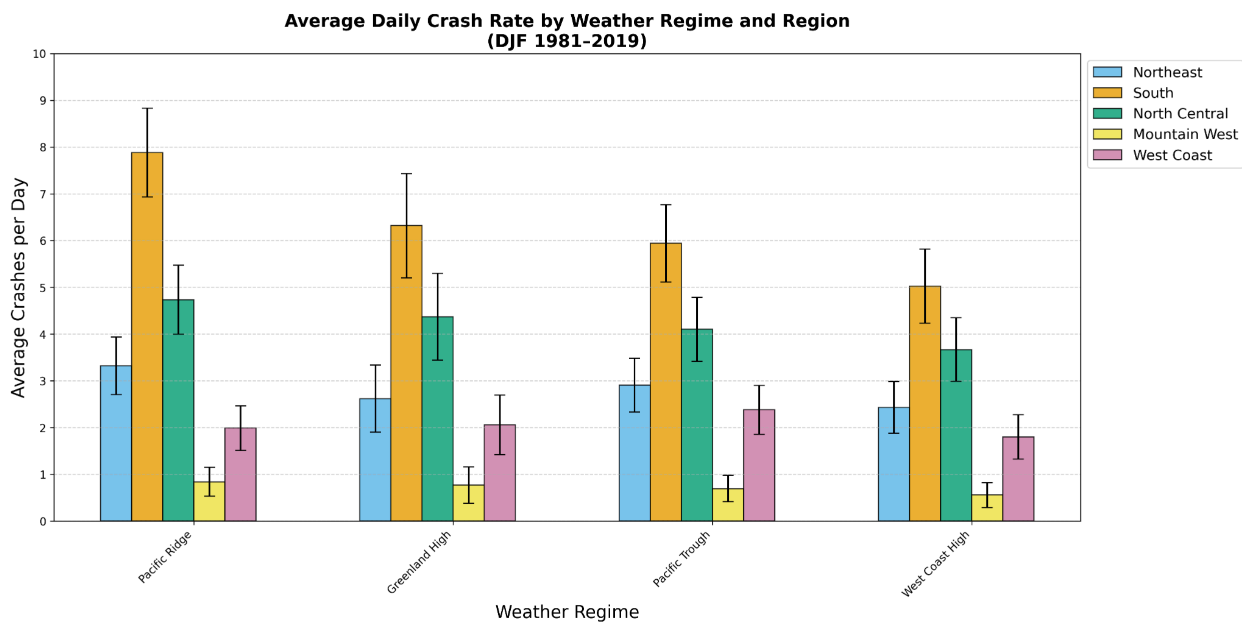

Figure 19. Barplots of the Fatal Crash Rate by Weather Regime for each region in CONUS. The Weather Regime type is shown on the x-axis and the crashes per day are shown on the y-axis. The 95% confidence interval is shown on the top of each bar.

3.3.3 State-by-state Analysis

The relationship between fatal weather-related crashes and weather regimes is investigated on a state-by-state basis. This is determined by the percentages calculated from the total number of fatal weather-related crashes that occurred in each state during 1981-2019, and are not normalized by crashes per day (Figure 20-23). The percentages help determine which regime has the most frequent fatal weather-related crashes for each region. In the Mountain West, the largest percentage of crashes took place during a Pacific Trough for Nevada and Utah, while the rest of the region had the most crashes during the Pacific Ridge (Figure 20-23). In the North Central region, South Dakota, North Dakota, and Wisconsin have the majority of their crashes occur during the Pacific Trough while the majority occurred during the Pacific Ridge for the rest of the states in the region (Figures 20 and 22). In the West Coast, the majority of crashes occur during the Pacific Trough for all states, while the largest percentage of crashes occur during the Pacific Ridge for all states in the Northeast and Southern regions (Figure 20 and 22). During a West Coast High or a Greenland High, the crash percentages are generally the lowest nationwide, with the largest percentage being 29.0% during a West Coast High for West Virginia and 27.6% for Nebraska (Figures 21 and 23).

When analyzing the three most populated states in CONUS (Texas, California, and Florida), the average crashes per day was found to be about 1.5 for Texas, 1.3 for California, and 0.8 for Florida during a Pacific Ridge. In Texas and Florida, this is a period where the largest average crashes per day occur, while the value is largest during a Pacific Trough regime for California (Figure 24). The confidence intervals indicate that the significant difference in average crashes per day varies greatly. The average crashes per day has the least overlap between the Pacific Ridge and the West Coast High for Texas at an alpha of 5%. This indicates that there may be some important difference between both regimes. In California, there is a more pronounced overlap between the Pacific Trough and Greenland High regimes with the Pacific Ridge and West Coast High regimes. This indicates that statistical differences are unlikely between the average crashes per day during each regime in California. In Florida, bars overlap almost entirely from regime to regime, indicating that there is seldom statistical difference between the average crashes per day during each regime in this state.

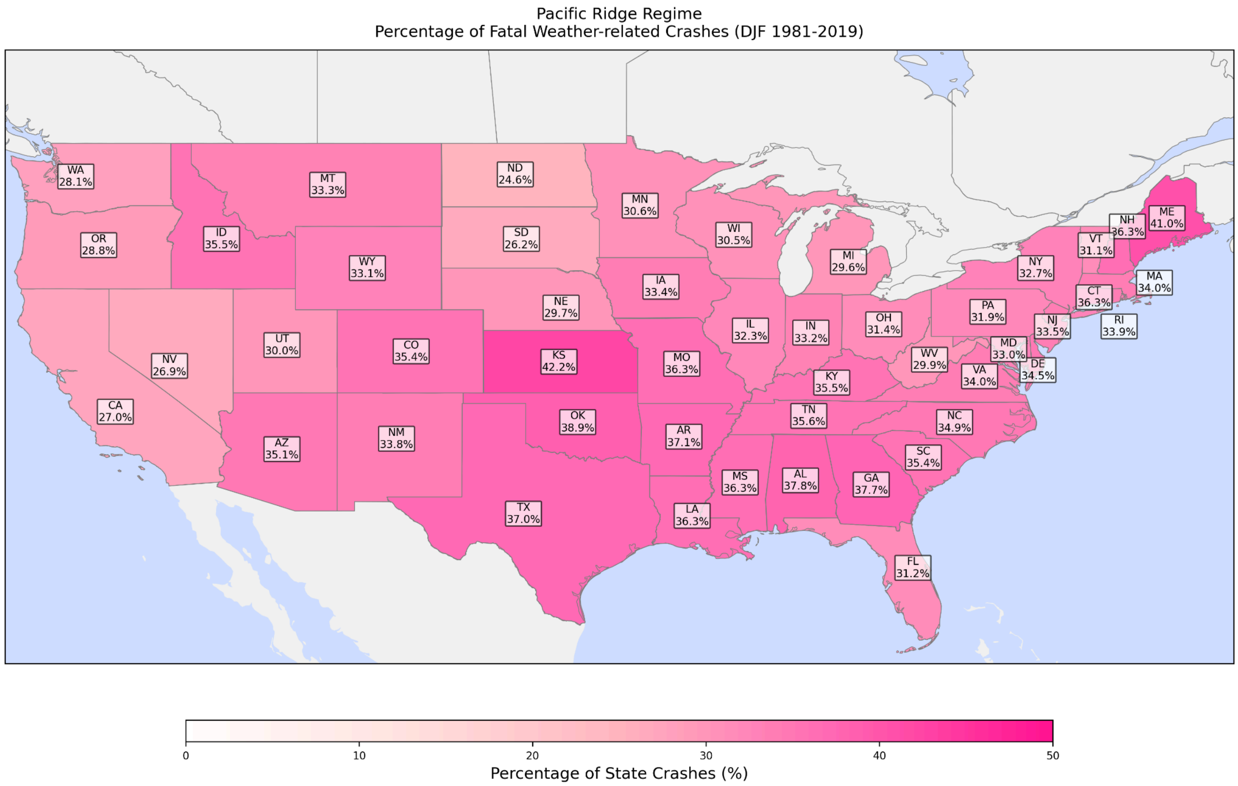

Figure 20. Map of the fatal weather-related crash percentage from total for each state during a Pacific Ridge regime.

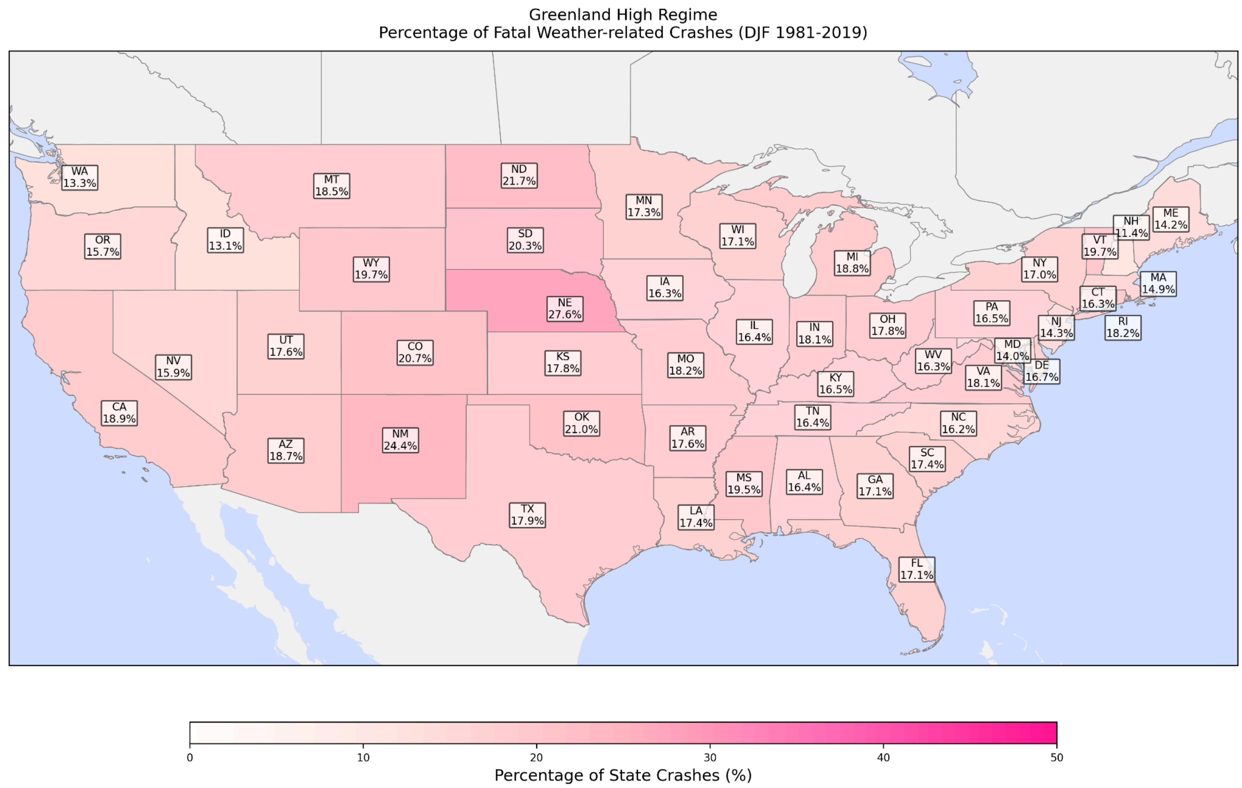

Figure 21. Map of the fatal weather-related crash percentage from total for each state during a Greenland High regime.

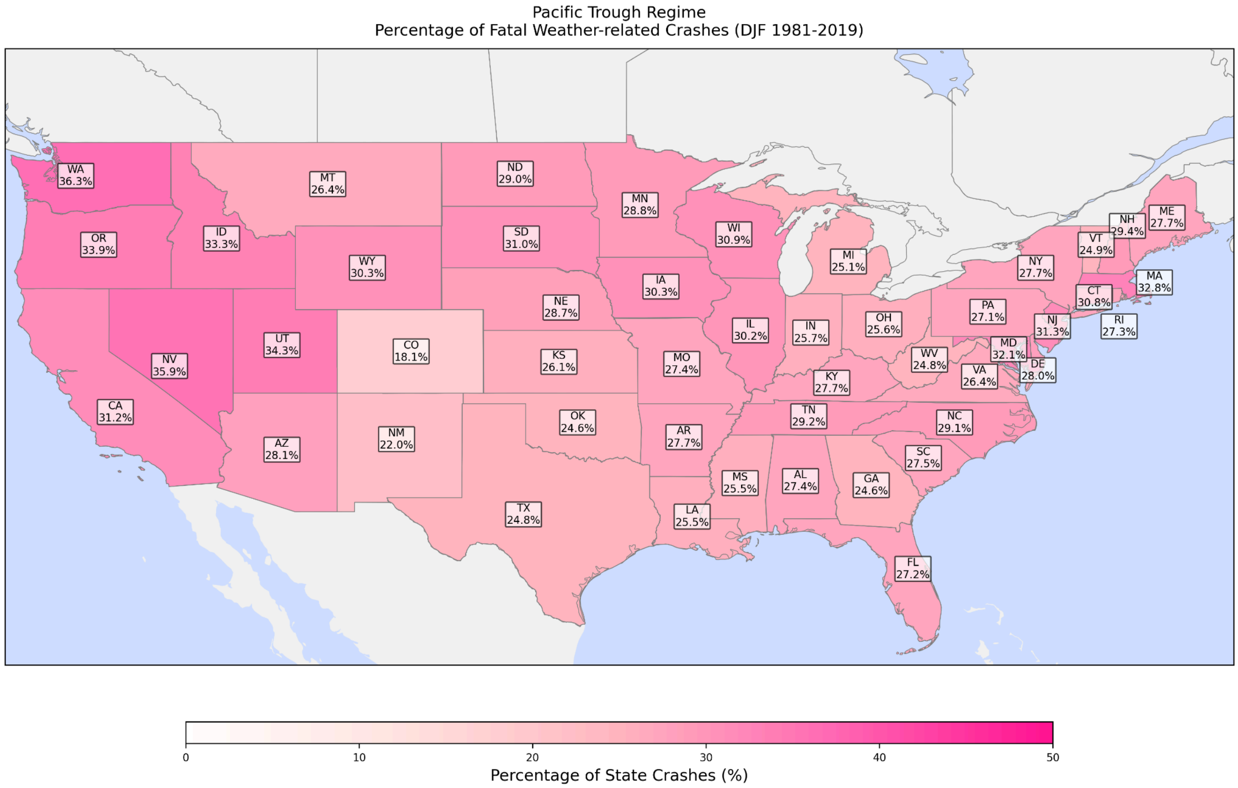

Figure 22. Map of the fatal weather-related crash percentage from total for each state during a Pacific Trough regime.

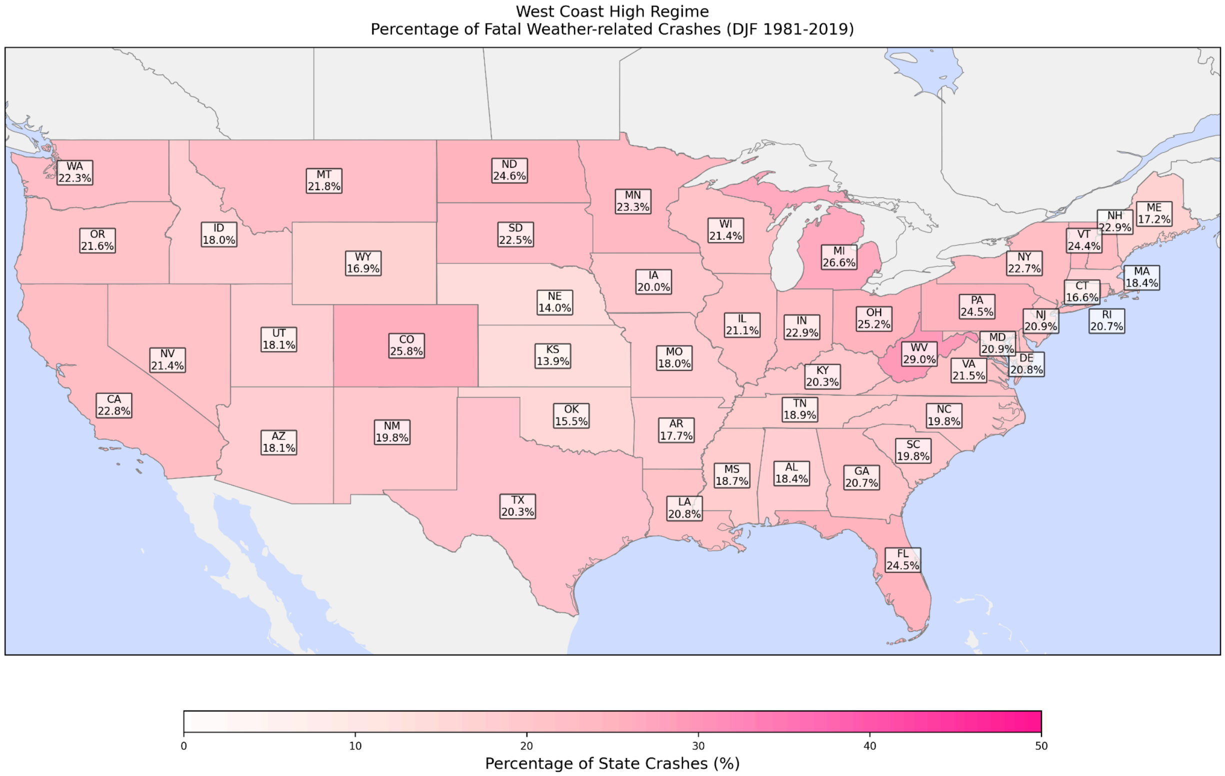

Figure 23. Map of the fatal weather-related crash percentage from total for each state during a West Coast High regime.

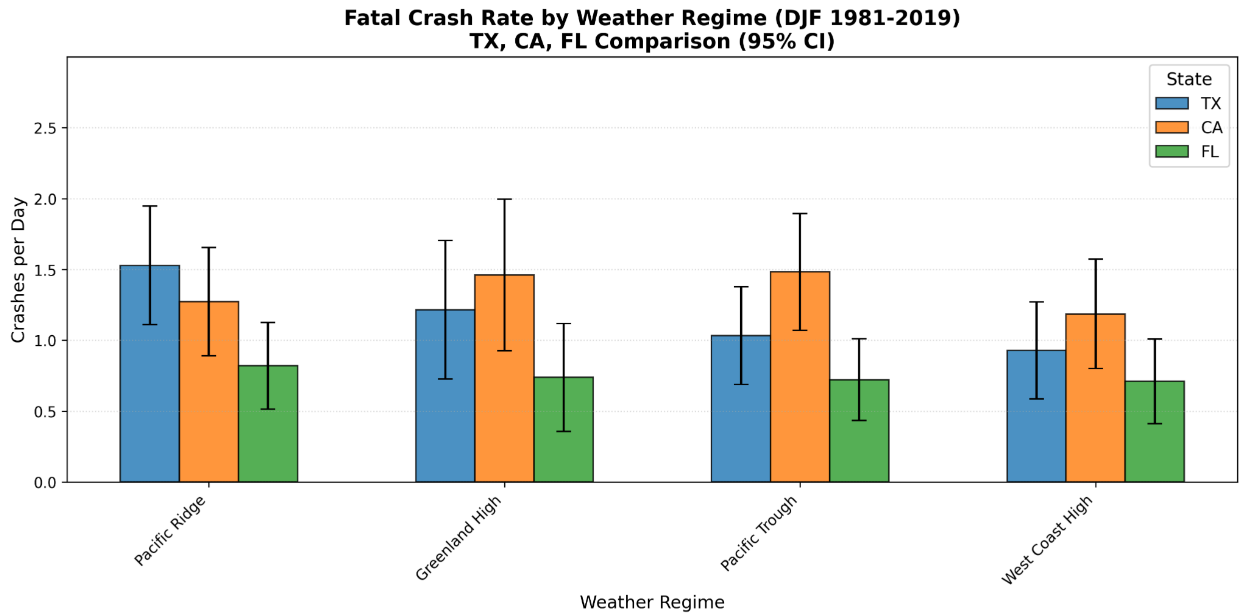

Figure 24. Barplots of the Fatal Crash Rate by Weather Regime for Texas, California, and Florida. The confidence interval is shown on the top of each bar.

CHAPTER 4: DISCUSSIONS AND CONCLUSIONS

The goal of this work is to investigate how seasonal to interannual precipitation variability associated with ENSO and subseasonal precipitation variability associated with weather regimes relate to fatal weather-related automobile crashes. A database was created by extracting and combining the Niño 3.4, CHIRPS, SWE, Weather Regime, and weather-related FARS data. A unique contribution of this study is that it investigates precipitation variability and its impact on FWRCA due to ENSO and weather regimes by state and/or state defined regions, making the results applicable to local, state, and federal transportation agencies. The results confirm that precipitation anomalies in each state are highly related to fatal weather-related crashes, but that this relationship is not due to the ENSO-related precipitation anomalies. The strongest relationship between precipitation anomalies and FWRCA occurs in California (R^2=~0.48) and Arizona (R^2=~0.45). The relationship between SWEA and FWRCA reveals that the relationship between precipitation anomalies and FWRCA is driven primarily by anomalous liquid precipitation rather than anomalous snow or frozen precipitation since this relationship is small in most states. The one exception is California where the SWEA and FWRCA have a R^2 value of 0.36 indicating that in CA, both frozen and liquid precipitation anomalies are related to FWRCA.

The intersection of weather regimes and fatal crash occurrence has not been previously investigated and provides insights on subseasonal precipitation variability and potential impacts on road safety. The Pacific Ridge regime occurs most frequently and was also associated with the highest number of fatal weather-related crashes over CONUS and the five regions even when normalized by the number of days in the regime. This is because there are strong positive precipitation anomalies in the Southern, North Central, and Northeast regions during this regime, despite strong negative precipitation anomalies in the West Coast (Figure 11). When the relationship is stratified by state, California, Nevada, North Dakota, Oregon, South Dakota, Washington, Wisconsin, and Utah have the highest average number of crashes per day during the Pacific Trough (Figures 22 and 24). This is a period where the precipitation anomalies are positive for the majority of the United States, with the strongest values being in the West Coast (Figure 11). The regime that was associated with the least fatal weather-related crashes was the West Coast High and this was true for all the defined regions in CONUS. While the West Coast High and the Greenland High periods may not be the regimes with the highest crash frequency in any region, they still impact overall precipitation anomalies. The Greenland High results in drier than normal conditions in the West Coast, while the West Coast High results in drier than normal conditions throughout the United States (Figure 11). State DOTs and weather-related agencies can use this information to better deliver advanced safety information to the public. For example, knowledge of what weather regime is occurring and its potential to persist could help agencies to prepare for hazardous road conditions in areas that are prone to conditions that result in fatal weather-related crashes, such as rain and snow. It could also provide information on the potential for an extended period of less hazardous road conditions which may allow for road safety improvements.

4.1 Total Precipitation Anomalies and Crash Implications

The strongest relationship between total precipitation anomalies and FWRCA were mostly scattered in the West Coast, the South, and the Mountain West. The former two regions have areas that receive a large amount of rain, while others receive little. Specifically for the

West Coast states, cities such as Ocean Shores, Washington receive as much as 254 cm (100 in) of rain per year, while others receive less than 25 cm (10 in), such as Bakersfield, California. Drivers that live in drier cities such as Bakersfield may be less experienced with driving during the rain than those in Ocean Shoes. This can indicate the need for improved safety communication for these areas, since commuters could potentially be inexperienced with driving during the rain in roads that are not designed to drain excess rainfall, therefore increasing the fatal crash occurrence.

Comparing SWEA and FWRCA is a fundamental way of determining how winter-related precipitation impacts crash occurrence, especially in snow-prone regions. The results showed that the strongest relationship between both variables were in California and Nevada, which contain regions that either receive a large amount of snow or none at all. However, the SWEA used were from SNODAS without considering its accuracy. Specifically in California, previous work has looked at the spatial variability of SWE in the Sierra Nevada using not only SNODAS data, but blended and reconstructed SWE data as well. The reconstructed SWE was made by taking spectral surface reflectance observations by the Moderate Resolution Imaging Spectroradiometer (MODIS) instrument, and blended SWE adjusts the reconstructed SWE using sensor data. While the findings of previous studies found that blended SWE is much more accurate than SNODAS, the lack of access to ground sensor data makes it difficult to use blended SWE with FWRCA (Guan et al. 2013; Gan et al. 2022). Even then, the use of any type of SWE with FWRCA has been seldom researched.

4.2 ENSO-related Precipitation and Crash Implications

Despite the fact that precipitation variability is impacted by teleconnections such as ENSO, its relationship with crashes is relatively weak. For example, California showed no linear relationship between ENSO-related precipitation and FWRCA, despite being a state that is known to be greatly impacted by ENSO. However, it is important to note that ENSO impacts each part of California differently. They can greatly impact the state by driving floods and droughts during an El Niño in the south and north, respectively (Schimmelmann et al. 1998, Schimmelmann et al. 2003, Du et al. 2020). Southern California typically expects colder and wetter winters during an El Niño, while northern California expects drier and warmer winters during the same ENSO phase. Central California is typically not impacted by ENSO. When taking the FWRCA for the entire state, this can obscure the actual relationship between ENSO and FWRCA in some areas of California. Taking California's data as a whole shows that while precipitation does impact FWRCA, it is not necessarily due to ENSO. This conflates low impact areas of the state with high impact areas of the state, leading to low correlations between ENSO and California's precipitation, a state where lower latitudes get more annual rainfall during an El Niño, while higher latitudes get less annual rainfall for that same event. To contrast, ENSO can reduce annual rainfall in the north, reducing the occurrence of a fatal crash. Additionally, there may be non-linear relationships worth future exploration as well.

4.3 Weather Regime and Crash Implications

This work used four defined weather regimes (identified by k-means clustering) with FARS, Precipitation, and ENSO data to investigate when and where fatal weather-related crashes are more frequent. The regime analysis provides evidence that precipitation variability impacts vehicle crashes spatially and temporally. The fatal crash occurrence is higher during the Pacific Ridge regime. Regionally, the occurrence of FWRCA was the highest during the Pacific Trough on the West Coast (Figure 22). During the West Coast High regime, the least number of crashes per day occurred for all regions (Figure 23). This can be attributed to the negative composite precipitation anomalies in this regime for most of CONUS. There were two states in the Mountain West (specifically Nevada and Utah), which were dominated by the Pacific Trough (35.9% for Nevada and 34.3% for Utah) instead of the Pacific Ridge like the rest of the region (Figures 20 and 22). This may be due to the fact that some positive or negative precipitation composite anomalies can bleed into a state that borders or is near a different region. Such is true for Nevada, which is just next to the West Coast Region, and Utah, which is right next to Nevada. This indicates that such an analysis may be more useful on a state-by-state basis. This is challenging to accomplish since county-specific precipitation and FARS data are not easily accessible. However, such data may exist internally and state DOTs as well as weather-related government agencies could use this information to better deliver road safety information to the public.

Every fatal crash that occurs can have major socioeconomic impacts which includes emergency response, safety, and insurance. Despite the differences of the frequency of crashes per day by state being small between regimes, they provide a direction where policy making should be more focused. The majority of fatal weather-related crashes occur during a Pacific Ridge nationwide except for the West Coast region, where most crashes occur during a Pacific Trough. This indicates that public communication from DOTs and weather agencies should be prioritized on days where the Pacific Trough regime is occurring for the West Coast as opposed to the rest of the nation, especially when California, the most populated state in the United States, resides in the West Coast. This is not to say that public communication is not important for less populated states, but rather that the timing and accuracy of communication is important.

4.4 Limitations

The analysis consisted of FWRCA that included all crashes that occurred during not only rain and snow, but fog, severe winds, and blowing dust. This data was not filtered to only include liquid and precipitation. However, the number of fatal weather-related crashes not due to precipitation is relatively small. Additionally, the crash data was not detrended, which may have been useful for uncovering patterns that were not initially seen with the trended data. The non-linear relationships were also not explored, which may also help with finding additional patterns from within the data. Human-related impacts such as changes in annual population, traffic duration, and improved traffic flow vary greatly over time. While the monthly anomalies calculated for the fatal weather-related crash data help identify trends clearly, this did not account for the change in the total population of the United States year after year. This is an additional parameter that can be normalized to better show that fatal weather-related crashes have been declining in recent years, whether it would be due to driver behavior or improved policy making.

4.5 Future Work

There is potential to further expand this work outside of the United States. In Europe, there are four defined Euro-Atlantic weather regimes that evolve year after year: The NAO+ (Positive North Atlantic Oscillation), NAO- (Negative North Atlantic Oscillation), Blocking, and the Atlantic Ridge (Cortesi et al. 2021). Like in this study, each of the European weather regimes can be assigned to a day, and if crash data is easily accessible, similar analyses can be performed. This will give a complete representation of how weather-regimes impact traffic conditions across the globe. Moreover, global transportation agencies can use such analyses to improve traffic safety in their region looking at weather regimes and ENSO provides a very useful concept in incorporating a range of teleconnections without having to define them (Lee et al. 2023). The NAO- aligns well with the Greenland High regime used in this work, and other teleconnections such as the Pacific North American (PNA) aligns with the effects of a Pacific Ridge or Pacific Trough (Lee et al. 2023). Both of these teleconnections influence weather in the West Coast and Northeast regions of the United States, which can potentially impact crash patterns.

To improve the accuracy of the SWEA and FWRCA relationship, blended SWE data can be used instead of the SNODAS SWE, since the former has been confirmed to be more accurate (Guan et al. 2013; Gan et al. 2022). However, this is strongly dependent on the availability of ground sensor and MODIS data in mountain regions of the United States. Afterwards, a comparative analysis between the reconstructed, blended, and SNODAS SWEA with FWRCA can be made possible. This can help confirm if different SWE data shows different results regarding the relationship with fatal weather-related vehicle crashes. There was also no publicly available SWE data from before 2003. If earlier data can be used for SWE, the more accurate its relationship with crashes will be.

Since fatal weather-related crashes only make up for a small fraction of all crashes, looking at all weather-related crash data (both fatal and non-fatal) can be useful for expanding the scope of this work. This increases the sample size substantially, which provides a clear picture to where most weather-related crashes occur. It is important to note that not all states have their respective crash data available to the public. Since there is not a singular source to get total crash data for every state, this data would need to be gathered individually from every state DOT.

REFERENCES

Amini, S., & Straus, D. M. (2019). Control of Storminess over the Pacific and North America by Circulation Regimes: The role of large-scale dynamics in weather extremes. *Climate Dynamics*, *52*(7–8), 4749–4770. https://doi.org/10.1007/s00382-018-4409-7

Andreescu, M., & Frost, D. (1998). Weather and traffic accidents in Montreal, Canada. *Climate Research*, *9*, 225–230. https://doi.org/10.3354/cr009225

Andrey, J. (2010). Long-term trends in weather-related crash risks. *Journal of Transport Geography*, *18*(2), 247–258. https://doi.org/10.1016/j.jtrangeo.2009.05.002

Ashley, W. S., Strader, S., Dziubla, D. C., & Haberlie, A. (2015). Driving Blind: Weather-Related Vision Hazards and Fatal Motor Vehicle Crashes. *Bulletin of the American Meteorological Society*, *96*(5), 755–778. https://doi.org/10.1175/BAMS-D-14-00026.1

Black, A. W., & Mote, T. L. (2015). Effects of winter precipitation on automobile collisions, injuries, and fatalities in the United States. *Journal of Transport Geography*, *48*, 165–175. https://doi.org/10.1016/j.jtrangeo.2015.09.007

Bunge, L., & Clarke, A. J. (2009). A Verified Estimation of the El Niño Index Niño-3.4 since 1877. *Journal of Climate*, *22*(14), 3979–3992. https://doi.org/10.1175/2009JCLI2724.1

Call, D. A., & Flynt, G. A. (2022). The Impact of Snowfall on Crashes, Traffic Volume, and Revenue on the New York State Thruway. *Weather, Climate, and Society*, *14*(1), 131–141. https://doi.org/10.1175/WCAS-D-21-0074.1

Call, D. A., Medina, R. M., & Black, A. W. (2019). Causes of Weather-Related Crashes in Salt Lake County, Utah. *The Professional Geographer*, *71*(2), 253–264. https://doi.org/10.1080/00330124.2018.1501713

Cassou, C., Terray, L., Hurrell, J. W., & Deser, C. (2004). North Atlantic Winter Climate Regimes: Spatial Asymmetry, Stationarity with Time, and Oceanic Forcing. *Journal of Climate*, *17*(5), 1055–1068. https://doi.org/10.1175/1520-0442(2004)017<1055:NAWCRS>2.0.CO;2

Cortesi, N., Torralba, V., Lledó, L., Manrique-Suñén, A., Gonzalez-Reviriego, N., Soret, A., & Doblas-Reyes, F. J. (2021). Yearly evolution of Euro-Atlantic weather regimes and of their sub-seasonal predictability. *Climate Dynamics*, *56*(11–12), 3933–3964. https://doi.org/10.1007/s00382-021-05679-y

Datla, S., & Sharma, S. (2008). Impact of cold and snow on temporal and spatial variations of highway traffic volumes. *Journal of Transport Geography*, *16*(5), 358–372. https://doi.org/10.1016/j.jtrangeo.2007.12.003

Du, X., Hendy, I., Hinnov, L., Brown, E., Schimmelmann, A., & Pak, D. (2020). Interannual Southern California Precipitation Variability During the Common Era and the ENSO Teleconnection. *Geophysical Research Letters*, *47*(1), e2019GL085891. https://doi.org/10.1029/2019GL085891

Eisenberg, D., & Warner, K. E. (2005). Effects of Snowfalls on Motor Vehicle Collisions, Injuries, and Fatalities. *American Journal of Public Health*, *95*(1), 120–124. https://doi.org/10.2105/AJPH.2004.048926

Elyoussoufi, A., Walker, C. L., Black, A. W., & DeGirolamo, G. J. (2023). The Relationships between Adverse Weather, Traffic Mobility, and Driver Behavior. *Meteorology*, *2*(4), 489–508. https://doi.org/10.3390/meteorology2040028

European Centre for Medium-Range Weather Forecasts (ECMWF), Copernicus Climate Change Service (C3S). (2021). ERA5 reanalysis: Weather regime data. https://cds.climate.copernicus.eu

Federal Highway Administration. (2025). How do weather events impact roads? U.S. Department of Transportation. https://ops.fhwa.dot.gov/weather/q1_roadimpact.htm

Fountas, G., Fonzone, A., Gharavi, N., & Rye, T. (2020). The joint effect of weather and lighting conditions on injury severities of single-vehicle accidents. *Analytic Methods in Accident Research*, *27*, 100124. https://doi.org/10.1016/j.amar.2020.100124

Francis, J. A., Skific, N., & Vavrus, S. J. (2018). North American Weather Regimes Are Becoming More Persistent: Is Arctic Amplification a Factor? *Geophysical Research Letters*, *45*(20). https://doi.org/10.1029/2018GL080252

Funk, C., Peterson, P., Landsfeld, M., Pedreros, D., Verdin, J., Shukla, S., Husak, G., Rowland, J., Harrison, L., Hoell, A., & Michaelsen, J. (2015). The climate hazards infrared precipitation with stations—A new environmental record for monitoring extremes. *Scientific Data*, *2*(1), 150066. https://doi.org/10.1038/sdata.2015.66

Gan, Y., Zhang, Y., Liu, Y., Kongoli, C., & Grassotti, C. (2022). Assimilation of blended in situ-satellite snow water equivalent into the National Water Model for improving hydrologic simulation in two US river basins. *Science of The Total Environment*, *838*, 156567. https://doi.org/10.1016/j.scitotenv.2022.156567

Guan, B., Molotch, N. P., Waliser, D. E., Jepsen, S. M., Painter, T. H., & Dozier, J. (2013). Snow water equivalent in the Sierra Nevada: Blending snow sensor observations with snowmelt model simulations. *Water Resources Research*, *49*(8), 5029–5046. https://doi.org/10.1002/wrcr.20387

Han, Z., & Sharif, H. O. (2020). Investigation of the Relationship between Rainfall and Fatal Crashes in Texas, 1994–2018. *Sustainability*, *12*(19), 7976. https://doi.org/10.3390/su12197976

Hansen, J. W., Hodges, A. W., & Jones, J. W. (1998). ENSO Influences on Agriculture in the Southeastern United States*. *Journal of Climate*, *11*(3), 404–411. https://doi.org/10.1175/1520-0442(1998)011<0404:EIOAIT>2.0.CO;2

Hersbach, H., Bell, B., Berrisford, P., Hirahara, S., Horányi, A., Muñoz‐Sabater, J., Nicolas, J., Peubey, C., Radu, R., Schepers, D., Simmons, A., Soci, C., Abdalla, S., Abellan, X., Balsamo, G., Bechtold, P., Biavati, G., Bidlot, J., Bonavita, M., Thépaut, J. (2020). The ERA5 global reanalysis. *Quarterly Journal of the Royal Meteorological Society*, *146*(730), 1999–2049. https://doi.org/10.1002/qj.3803

Huang, X., & Stevenson, S. (2023). Contributions of Climate Change and ENSO Variability to Future Precipitation Extremes Over California. *Geophysical Research Letters*, *50*(12), e2023GL103322. https://doi.org/10.1029/2023GL103322

Jackson, T. L., & Sharif, H. O. (2016). Rainfall impacts on traffic safety: Rain-related fatal crashes in Texas. *Geomatics, Natural Hazards and Risk*, *7*(2), 843–860. https://doi.org/10.1080/19475705.2014.984246

Kostis, H. (2019). *SVS: Niño 3.4 index and sea surface temperature anomaly timeline: 1982–2017*. NASA Scientific Visualization Studio. https://svs.gsfc.nasa.gov/4695

Kim, K., Chowdhury, R., Pant, P., Yamashita, E., & Ghimire, J. (2021). Assessment of ENSO risks to support transportation resilience. *Progress in Disaster Science*, *12*, 100196. https://doi.org/10.1016/j.pdisas.2021.100196

Kwon, T. J., Fu, L., & Jiang, C. (2013). Effect of Winter Weather and Road Surface Conditions on Macroscopic Traffic Parameters. *Transportation Research Record: Journal of the Transportation Research Board*, *2329*(1), 54–62. https://doi.org/10.3141/2329-07

Lee, S. H., Charlton‐Perez, A. J., Furtado, J. C., & Woolnough, S. J. (2020). Representation of the Scandinavia–Greenland pattern and its relationship with the polar vortex in S2S forecast models. *Quarterly Journal of the Royal Meteorological Society*, *146*(733), 4083–4098. https://doi.org/10.1002/qj.3892

Lee, S. H., Tippett, M. K., & Polvani, L. M. (2023). A New Year-Round Weather Regime Classification for North America. *Journal of Climate*, *36*(20), 7091–7108. https://doi.org/10.1175/JCLI-D-23-0214.1

Lobo, A., Ferreira, S., Iglesias, I., & Couto, A. (2019). Urban Road Crashes and Weather Conditions: Untangling the Effects. *Sustainability*, *11*(11), 3176. https://doi.org/10.3390/su11113176

Luojus, K., Pulliainen, J., Takala, M., Lemmetyinen, J., Mortimer, C., Derksen, C., Mudryk, L., Moisander, M., Hiltunen, M., Smolander, T., Ikonen, J., Cohen, J., Salminen, M., Norberg, J., Veijola, K., & Venäläinen, P. (2021). GlobSnow v3.0 Northern Hemisphere snow water equivalent dataset. *Scientific Data*, *8*(1). https://doi.org/10.1038/s41597-021-00939-2

Mills, B., Andrey, J., Doberstein, B., Doherty, S., & Yessis, J. (2019). Changing patterns of motor vehicle collision risk during winter storms: A new look at a pervasive problem. *Accident Analysis & Prevention*, *127*, 186–197. https://doi.org/10.1016/j.aap.2019.02.027

Molina, M. J., Richter, J. H., Glanville, A. A., Dagon, K., Berner, J., Hu, A., & Meehl, G. A. (2023). Subseasonal Representation and Predictability of North American Weather

Regimes Using Cluster Analysis. *Artificial Intelligence for the Earth Systems*, *2*(2), e220051. https://doi.org/10.1175/AIES-D-22-0051.1

Mo, K. C., & Schemm, J. E. (2008). Relationships between ENSO and drought over the southeastern United States. *Geophysical Research Letters*, *35*(15), 2008GL034656. https://doi.org/10.1029/2008GL034656

Huang, B., Thorne, P. W., Banzon, V. F., Boyer, T., Chepurin, G., Lawrimore, J. H., Menne, M. J., Smith, T. M., Vose, R. S., & Zhang, H.-M. (2017). NOAA Extended Reconstructed Sea Surface Temperature (ERSST), Version 5 [Data set]. NOAA National Centers for Environmental Information. https://doi.org/10.7289/V5T72FNM

National Operational Hydrologic Remote Sensing Center. (2004). Snow Data Assimilation System (SNODAS) Data Products at NSIDC (Version 1) [Data set]. National Snow and Ice Data Center. https://doi.org/10.7265/N5TB14TC

Obeidat, M. S., Obeidat, R. M., & Dweiri, F. (2024). Unravelling the veil of traffic safety: A comprehensive analysis of factors influencing crash frequency across US states. *Transportation Safety and Environment*, *6*(4), tdae016. https://doi.org/10.1093/tse/tdae016

Page, Y. (2001). A statistical model to compare road mortality in OECD countries. *Accident Analysis & Prevention*, *33*(3), 371–385. https://doi.org/10.1016/S0001-4575(00)00051-8

Patten, J. M., Smith, S. R., & O'Brien, J. J. (2003). Impacts of ENSO on Snowfall Frequencies in the United States. *Weather and Forecasting*, *18*(5), 965–980. https://doi.org/10.1175/1520-0434(2003)018<0965:IOEOSF>2.0.CO;2

Perrels, A., Votsis, A., Nurmi, V., & Pilli-Sihvola, K. (2015). Weather Conditions, Weather Information and Car Crashes. *ISPRS International Journal of Geo-Information*, *4*(4), 2681–2703. https://doi.org/10.3390/ijgi4042681

Pisano, P. A., Goodwin, L. C., & Rossetti, M. A. (2008, January). US highway crashes in adverse road weather conditions. In the 24th conference on international interactive information and processing systems for meteorology, oceanography and hydrology, New Orleans, LA (pp. 20-24).

Power, S., Delage, F., Chung, C., Kociuba, G., & Keay, K. (2013). Robust twenty-first-century projections of El Niño and related precipitation variability. *Nature*, *502*(7472), 541–545. https://doi.org/10.1038/nature12580

Reinhold, B. B., & Pierrehumbert, R. T. (1982). Dynamics of Weather Regimes: Quasi-Stationary Waves and Blocking. *Monthly Weather Review*, *110*(9), 1105–1145. https://doi.org/10.1175/1520-0493(1982)110<1105:DOWRQS>2.0.CO;2

Robertson, A. W., Vigaud, N., Yuan, J., & Tippett, M. K. (2020). Toward Identifying Subseasonal Forecasts of Opportunity Using North American Weather Regimes. *Monthly Weather Review*, *148*(5), 1861–1875. https://doi.org/10.1175/MWR-D-19-0285.1

Roh, H.-J., Datla, S., & Sharma, S. (2013). Effect of Snow, Temperature and Their Interaction on Highway Truck Traffic. *Journal of Transportation Technologies*, *03*(01), 24–38. https://doi.org/10.4236/jtts.2013.31003

Saha, S., Schramm, P., Nolan, A., & Hess, J. (2016). Adverse weather conditions and fatal motor vehicle crashes in the United States, 1994-2012. *Environmental Health*, *15*(1), 104. https://doi.org/10.1186/s12940-016-0189-x

Schimmelmann, A., Lange, C. B., & Meggers, B. J. (2003). Palaeoclimatic and archaeological evidence for a 200-yr recurrence of floods and droughts linking California, Mesoamerica and South America over the past 2000 years. *The Holocene*, *13*(5), 763–778. https://doi.org/10.1191/0959683603hl661rp

Schimmelmann, A., Zhao, M., Harvey, C. C., & Lange, C. B. (1998). A Large California Flood and Correlative Global Climatic Events 400 Years Ago. *Quaternary Research*, *49*(1), 51–61. https://doi.org/10.1006/qres.1997.1937

Schmidt, N., Lipp, E. K., Rose, J. B., & Luther, M. E. (2001). ENSO Influences on Seasonal Rainfall and River Discharge in Florida. *Journal of Climate*, *14*(4), 615–628. https://doi.org/10.1175/1520-0442(2001)014<0615:EIOSRA>2.0.CO;2

Schmidt, N., & Luther, M. E. (2002). ENSO impacts on salinity in Tampa Bay, Florida. *Estuaries*, *25*(5), 976–984. https://doi.org/10.1007/BF02691345

Seager, R., Harnik, N., Robinson, W. A., Kushnir, Y., Ting, M., Huang, H.-P., & Velez, J. (2005). Mechanisms of ENSO-forcing of hemispherically symmetric precipitation variability. *Quarterly Journal of the Royal Meteorological Society*, *131*(608), 1501–1527. https://doi.org/10.1256/qj.04.96

Stevens, S. E., Schreck, C. J., Saha, S., Bell, J. E., & Kunkel, K. E. (2019). Precipitation and Fatal Motor Vehicle Crashes: Continental Analysis with High-Resolution Radar Data. *Bulletin of the American Meteorological Society*, *100*(8), 1453–1461. https://doi.org/10.1175/BAMS-D-18-0001.1

Tobin, D. M., Kastman, J. S., Nelson, J. A., & Reeves, H. D. (2024a). Toward the Development of an Impact-Based Decision Support Tool for Surface-Transportation Hazards. Part I:

Tying Weather Variables to Road Hazards and Quantifying Impacts. *Weather and Forecasting*, *39*(8), 1117–1128. https://doi.org/10.1175/WAF-D-23-0219.1

Tobin, D. M., Kastman, J. S., Nelson, J. A., & Reeves, H. D. (2024b). Toward the Development of an Impact-Based Decision Support Tool for Surface-Transportation Hazards. Part II: An Hourly Winter Storm Severity Index. *Weather and Forecasting*, *39*(8), 1129–1142. https://doi.org/10.1175/WAF-D-23-0220.1

Tobin, D. M., Kumjian, M. R., & Black, A. W. (2019). Characteristics of Recent Vehicle-Related Fatalities during Active Precipitation in the United States. *Weather, Climate, and Society*, *11*(4), 935–952. https://doi.org/10.1175/WCAS-D-18-0110.

Tobin, D. M., Kumjian, M. R., & Black, A. W. (2021). Effects of precipitation type on crash relative risk estimates in Kansas. *Accident Analysis & Prevention*, *151*, 105946. https://doi.org/10.1016/j.aap.2020.105946

Tobin, D. M., Reeves, H. D., Gibson, M. N., & Rosenow, A. A. (2022). Weather Conditions and Messaging Associated with Fatal Winter-Weather-Related Motor-Vehicle Crashes. *Weather, Climate, and Society*, *14*(3), 835–848. https://doi.org/10.1175/WCAS-D-21-0112.1

Trenberth, K. E., & Stepaniak, D. P. (2001). Indices of El Niño Evolution. *Journal of Climate*, *14*(8), 1697–1701. https://doi.org/10.1175/1520-0442(2001)014<1697:LIOENO>2.0.CO;2

U.S. Census Bureau. (2024, October 30). Cartographic boundary files - Shapefile. https://www.census.gov/geographies/mapping-files/time-series/geo/carto-boundary-file.html

Wang, C., & Fiedler, P. C. (2006). ENSO variability and the eastern tropical Pacific: A review. *Progress in Oceanography*, *69*(2–4), 239–266. https://doi.org/10.1016/j.pocean.2006.03.004

Whitelegg, J. (1987). A Geography of Road Traffic Accidents. *Transactions of the Institute of British Geographers*, *12*(2), 161. https://doi.org/10.2307/622525

Wilson, F. A., & Stimpson, J. P. (2010). Trends in Fatalities From Distracted Driving in the United States, 1999 to 2008. *American Journal of Public Health*, *100*(11), 2213–2219. https://doi.org/10.2105/AJPH.2009.187179

Winters, A. C., & Walker, C. L. (2022). A Jet-Centered Framework for Investigating High Plains Winter Storm Severity. *Journal of Applied Meteorology and Climatology*, *61*(6), 709–728. https://doi.org/10.1175/JAMC-D-21-0211.1

Yan, L., He, Y., Qin, L., Wu, C., Zhu, D., & Ran, B. (2020). A novel feature extraction model for traffic injury severity and its application to Fatality Analysis Reporting System data analysis. *Science Progress*, *103*(1), 0036850419886471. https://doi.org/10.1177/0036850419886471

Yu, J., & Kim, S. T. (2013). Identifying the types of major El Niño events since 1870. *International Journal of Climatology*, *33*(8), 2105–2112. https://doi.org/10.1002/joc.3575